Four Vignettes

Frank Timmes

MESA

SPIDER

Starlib

JINA-CEE

100 isotopes project

edX

THE ASTROPHYSICAL JOURNAL

NSF

SIMONS FOUNDATION

NASA

Persistence of Memory

3D Element Factories

26 Modes of Uncertainty

The Short and Long of Paper Citations

Persistence of Memory

White dwarf supernova play a key role in astronomy:

Distance indicators

Element factories

Cosmic-ray accelerators

Kinetic energy sources

Binary star terminus

Identification of the progenitor system(s) remains unknown.
This is the outstanding mystery in the field.

Observed correlations between the peak and width of the light curve help in the hunt for the progenitors.

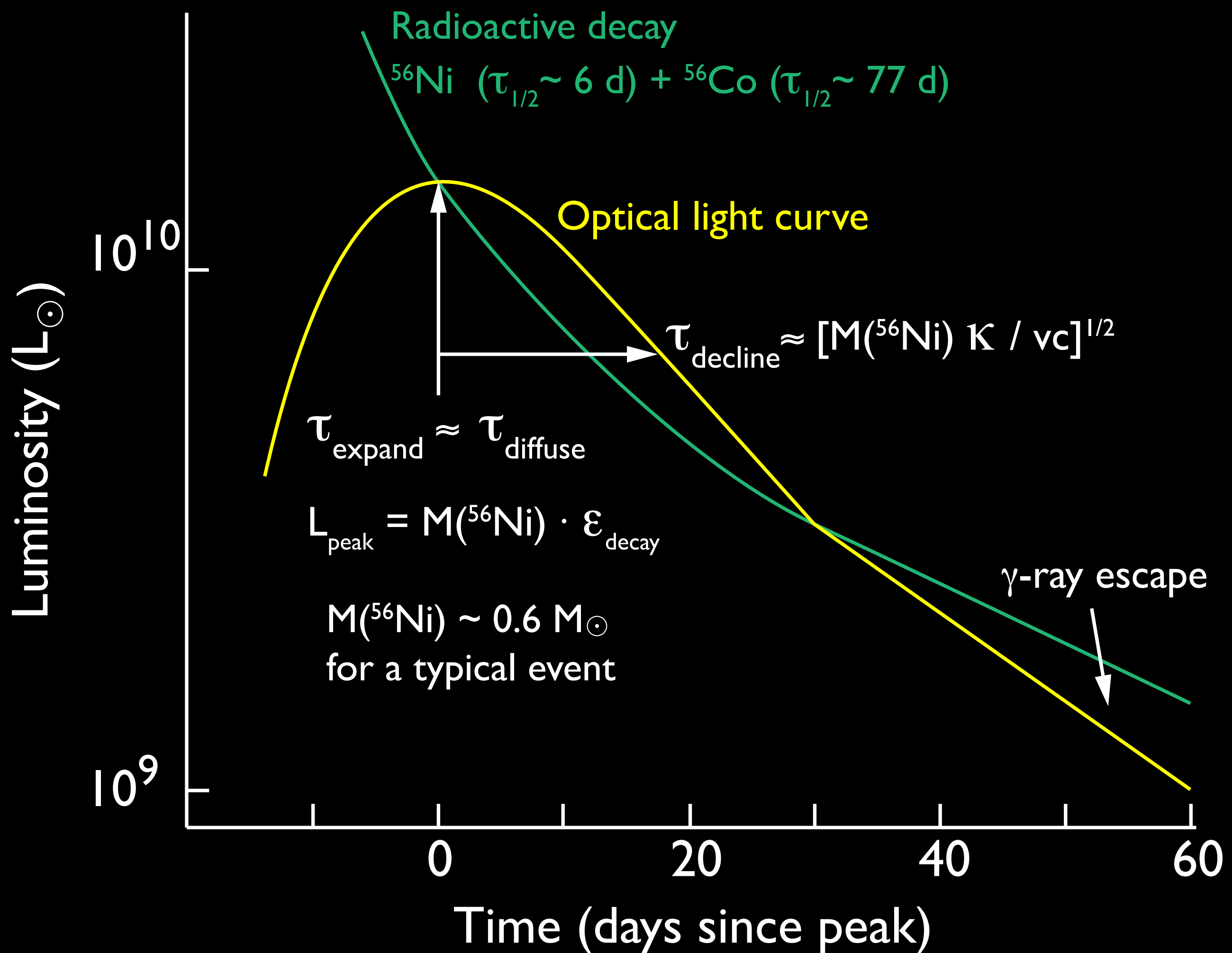

Radioactive decay
^{56}Ni ($\tau_{1/2}$~ 6 d) + ^{56}Co ($\tau_{1/2}$~ 77 d)
Optical light curve
$\tau_{decline} \approx [M(^{56}Ni)\ \kappa\ /\ vc]^{1/2}$
$\tau_{expand} \approx \tau_{diffuse}$
$L_{peak} = M(^{56}Ni) \cdot \varepsilon_{decay}$
M(^{56}Ni) ~ 0.6 $M_{\odot}$
for a typical event
γ-ray escape
10^{10}
10^{9}
Luminosity ($L_{\odot}$)
0
20
40
60
Time (days since peak)

Brighter is wider.

This empirical fact can be used to correct for variations in the peak luminosity to give a standard candle.

After correction, distances are accurate to ≤ 7% .

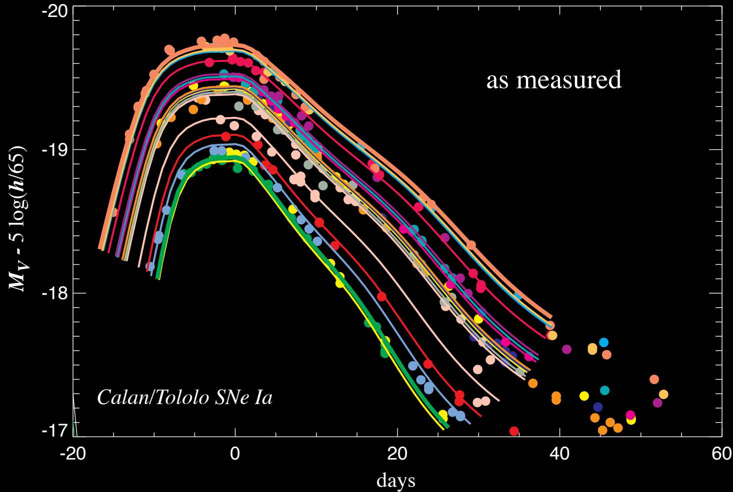

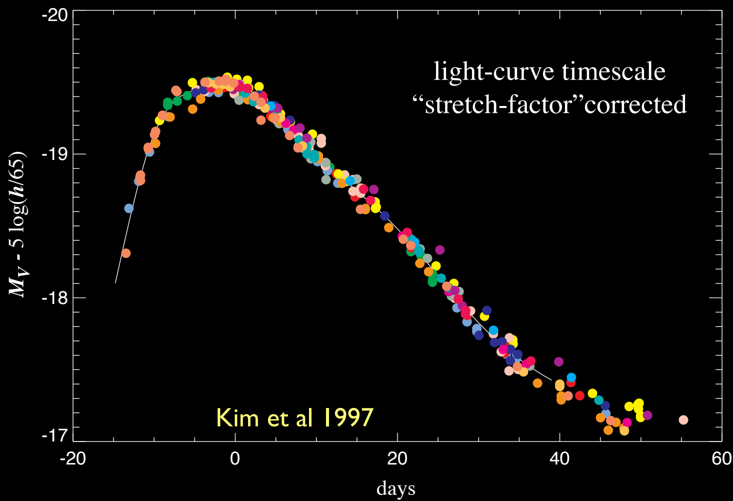

Variations in the peak luminosity may originate in part from a scatter in the composition of the main-sequence stars that become white dwarfs.

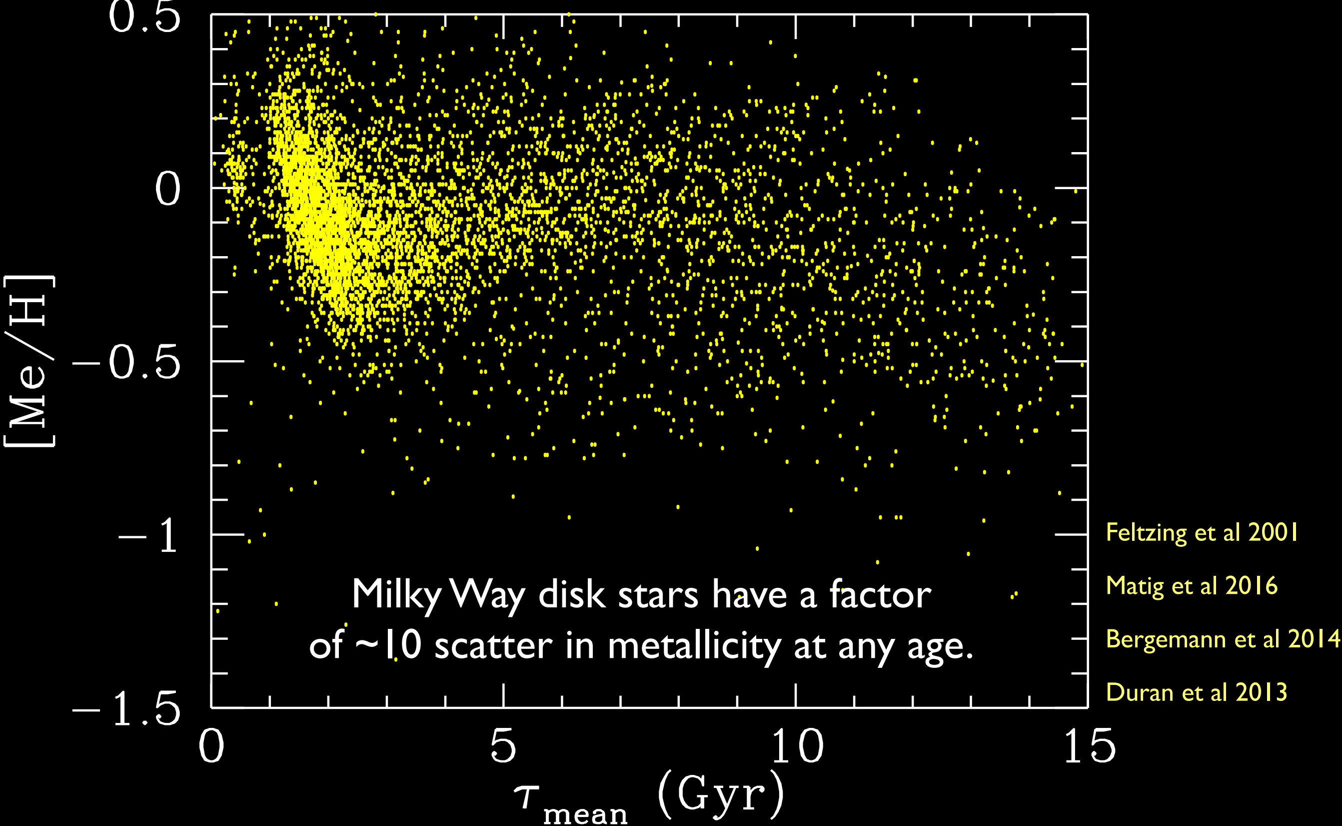

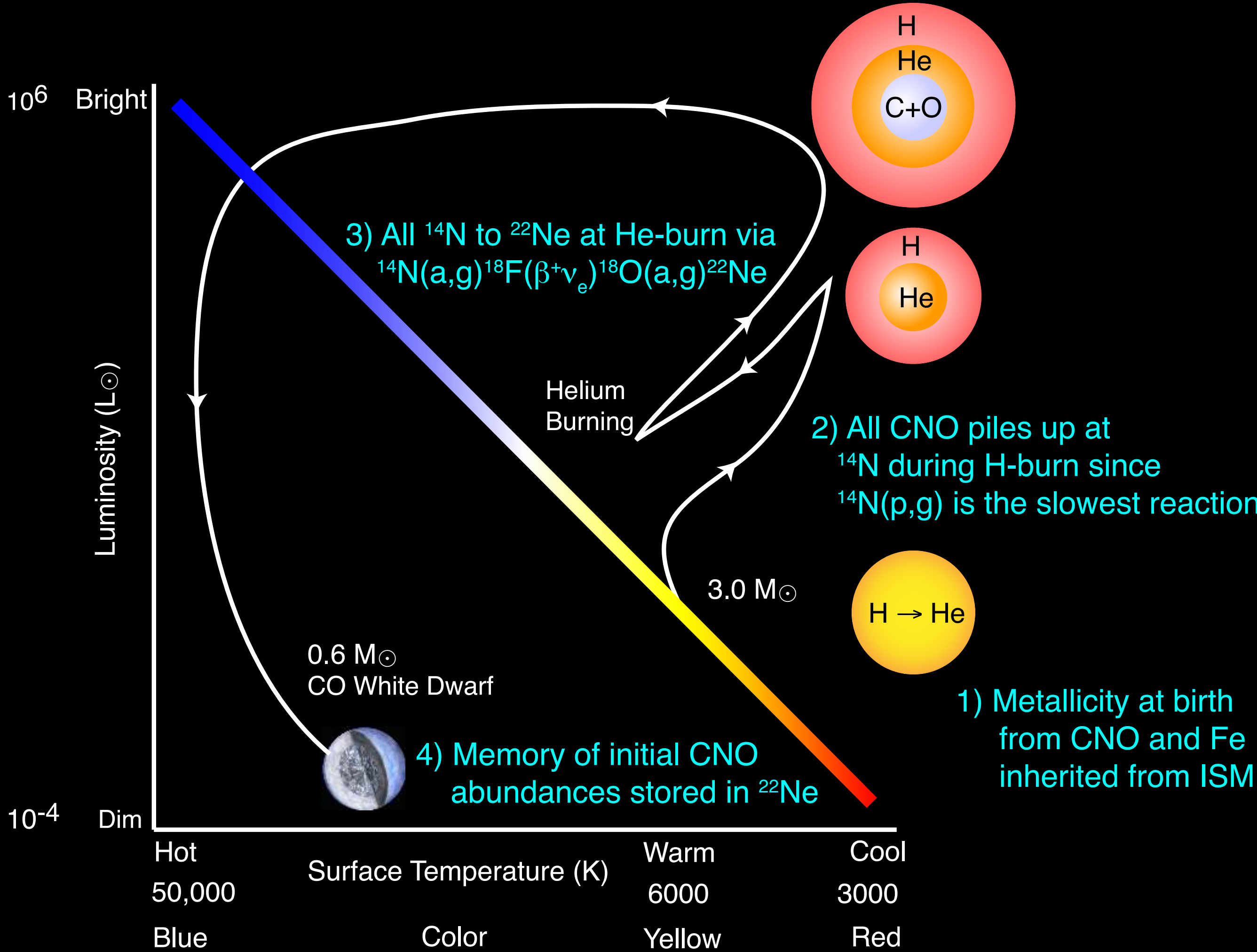

H
He
C+O
H
He
H → He
10^6 Bright
10^-4 Dim
Luminosity (L☉)
3) All ¹⁴N to ²²Ne at He-burn via
¹⁴N(a,g)¹⁸F(β⁺νe)¹⁸O(a,g)²²Ne
Helium
Burning
2) All CNO piles up at
¹⁴N during H-burn since
¹⁴N(p,g) is the slowest reaction
3.0 M☉
0.6 M☉
CO White Dwarf
4) Memory of initial CNO
abundances stored in ²²Ne
1) Metallicity at birth
from CNO and Fe
inherited from ISM
Hot
50,000
Blue
Surface Temperature (K)
Color
Warm
6000
Yellow
Cool
3000
Red

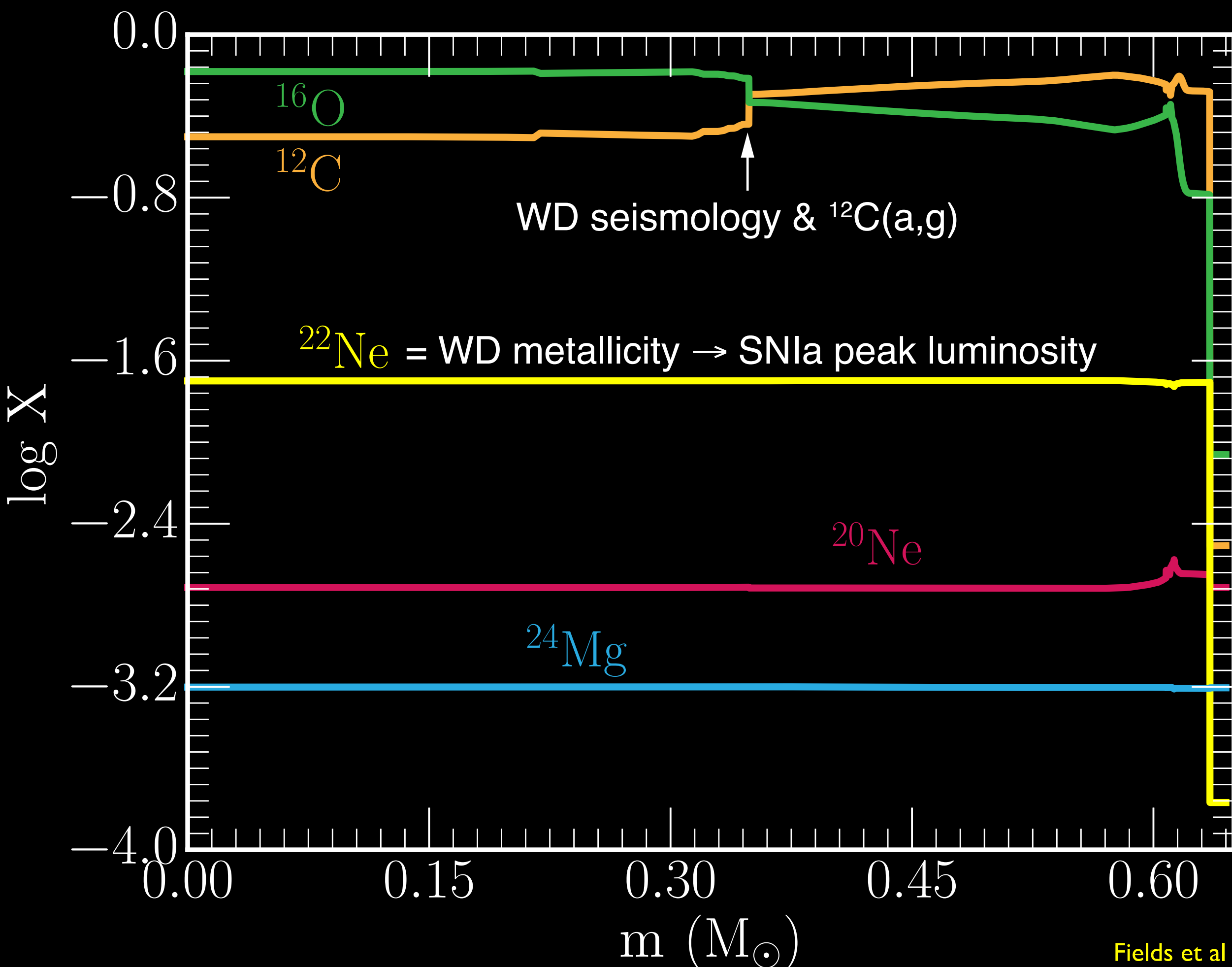

Fields et al 2016

Mass and charge conservation set the white dwarf's neutron enrichment:

$$\sum_{i=1}^{n} \mathrm{X}_i = 1 \qquad \mathrm{Y}_e = \sum_{i=1}^{n} \frac{\mathrm{Z}_i}{\mathrm{A}_i} \mathrm{X}_i$$

$$\mathrm{X}(^{22}\mathrm{Ne}) = 22 \left[\frac{\mathrm{X}(^{12}\mathrm{C})}{12} + \frac{\mathrm{X}(^{14}\mathrm{N})}{14} + \frac{\mathrm{X}(^{16}\mathrm{O})}{16} \right]$$

$$\mathrm{Y}_e = \frac{10}{22}\,\mathrm{X}(^{22}\mathrm{Ne}) + \frac{26}{56}\,\mathrm{X}(^{56}\mathrm{Fe}) + \frac{1}{2}\left[1 - \mathrm{X}(^{22}\mathrm{Ne}) - \mathrm{X}(^{56}\mathrm{Fe})\right]$$

^{56}Ni and ^{58}Ni are the dominant species produced by the explosion. Mass and charge conservation imply

$$X(^{56}\mathrm{Ni}) = 1 - X(^{58}\mathrm{Ni}) = 58\mathrm{Y}_e - 28$$

We can set Y_e equal to the initial Y_e of the white dwarf since weak interactions do not dominate where most of the ^{56}Ni is made:

$$\mathrm{X}(^{56}\mathrm{Ni}) = 1 - 0.057\frac{Z}{Z_\odot}$$

This relation connects a quantity at birth to a quantity at explosion.

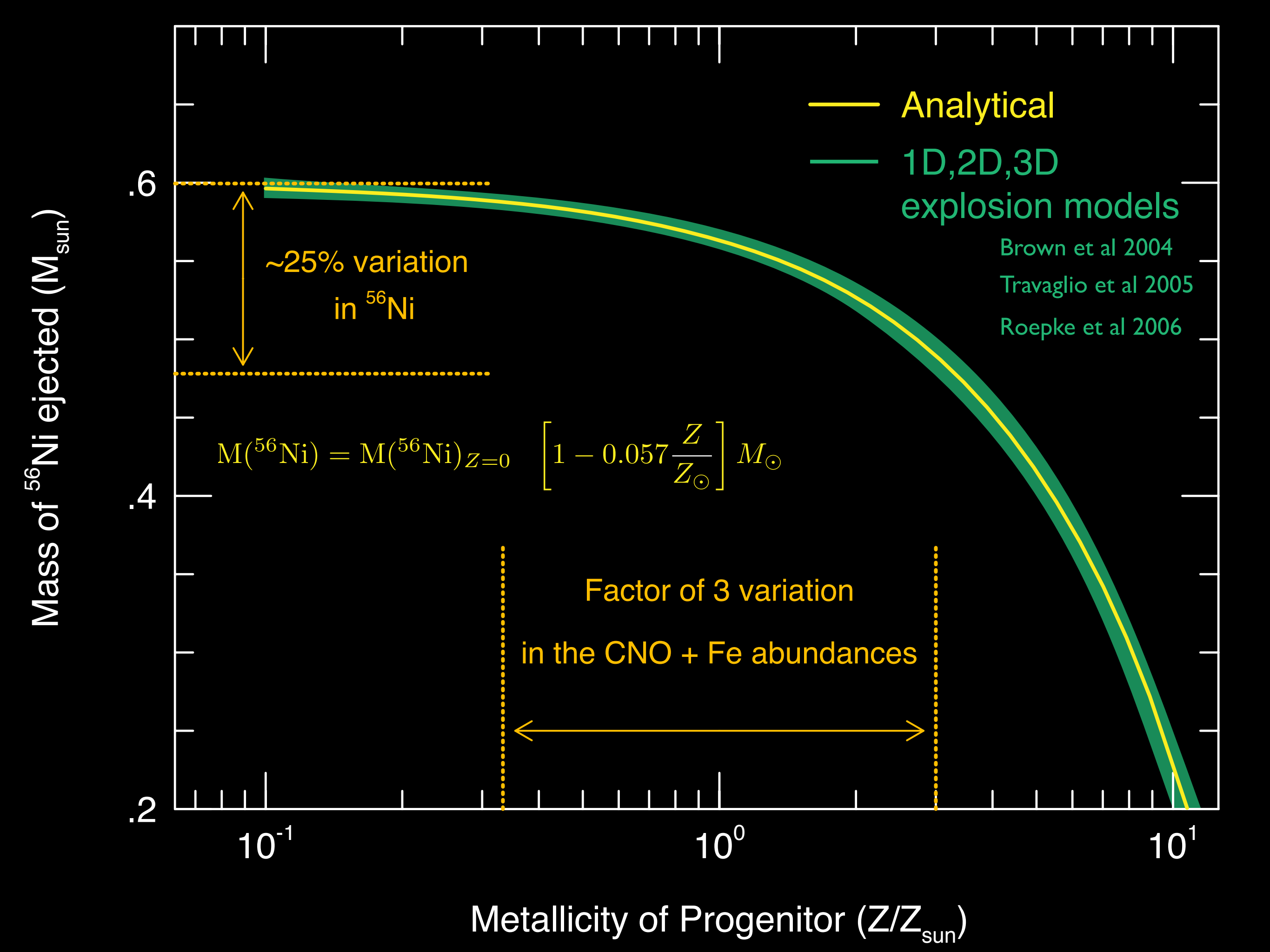
Analytical
1D,2D,3D
explosion models
Brown et al 2004
Travaglio et al 2005
Roepke et al 2006
~25% variation
in 56Ni
M(56Ni) = M(56Ni)Z=0 [1 − 0.057 Z/Z⊙] M⊙
Factor of 3 variation
in the CNO + Fe abundances
.6
.4
.2
10-1
100
101
Mass of 56Ni ejected (Msun)
Metallicity of Progenitor (Z/Zsun)

Observations find consistency with the analytical result.
Trend seems smaller than predicted, with considerable scatter.

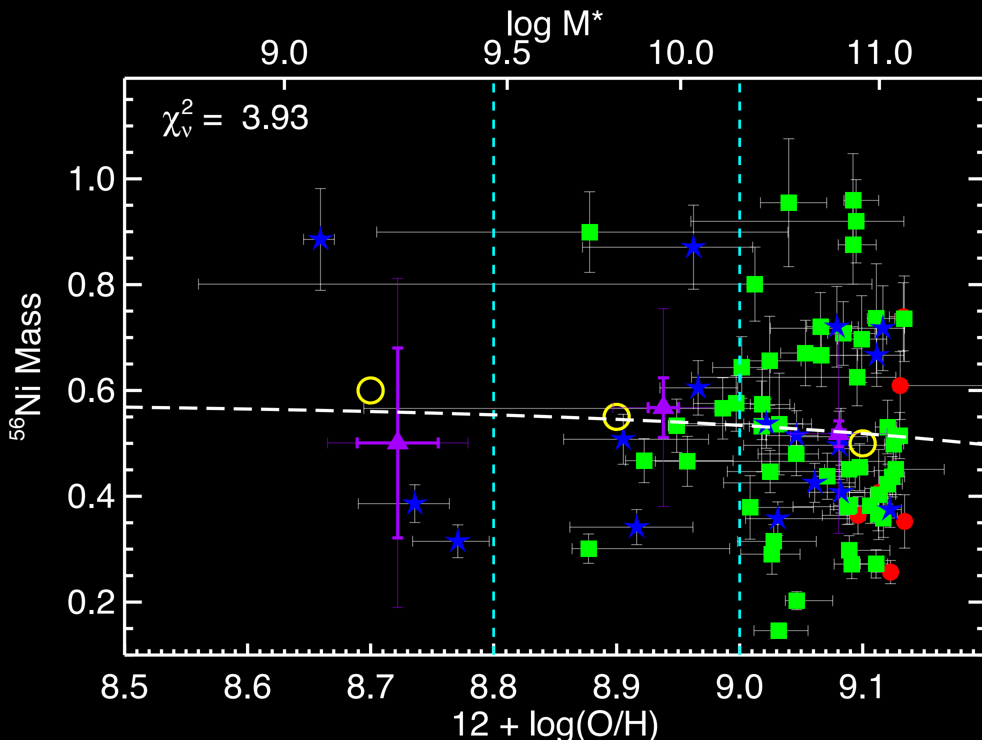

Neill et al 2009

Howell et al 2009

Gallagher et al 2008

Ellis et al 2007

Such efforts assume galaxy metallicity = supernova metallicity.

The Si-group elements are also affected by the white dwarf metallicity in a model independent manner.

^{28}Si is insensitive to Y_e,
^{32}S has a nearly linear trend,
^{40}Ca has a nearly quadratic trend.

Measurement of Y_{28Si}, Y_{32S}/Y_{28Si}, Y_{40Ca}/Y_{32S}, Y_{54Fe}/Y_{28Si} is a sufficient to determine Y_e to ~6%.

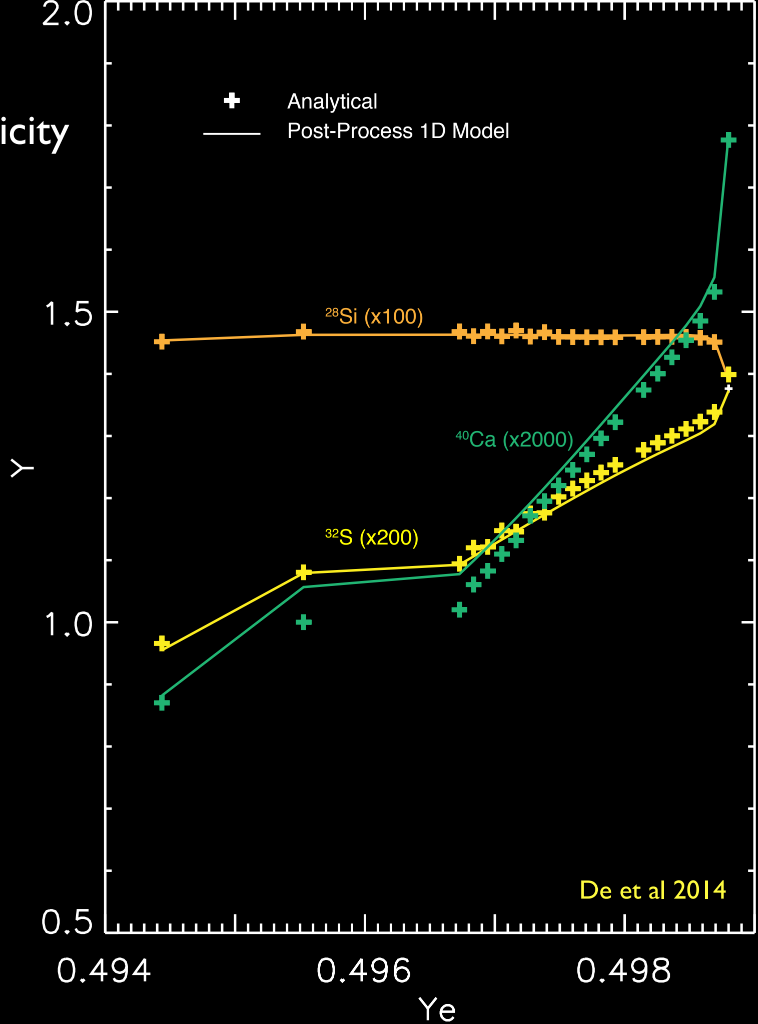

Supernova remnants suggest the Ca/S ratio is a robust tracer of white dwarf neutronization.

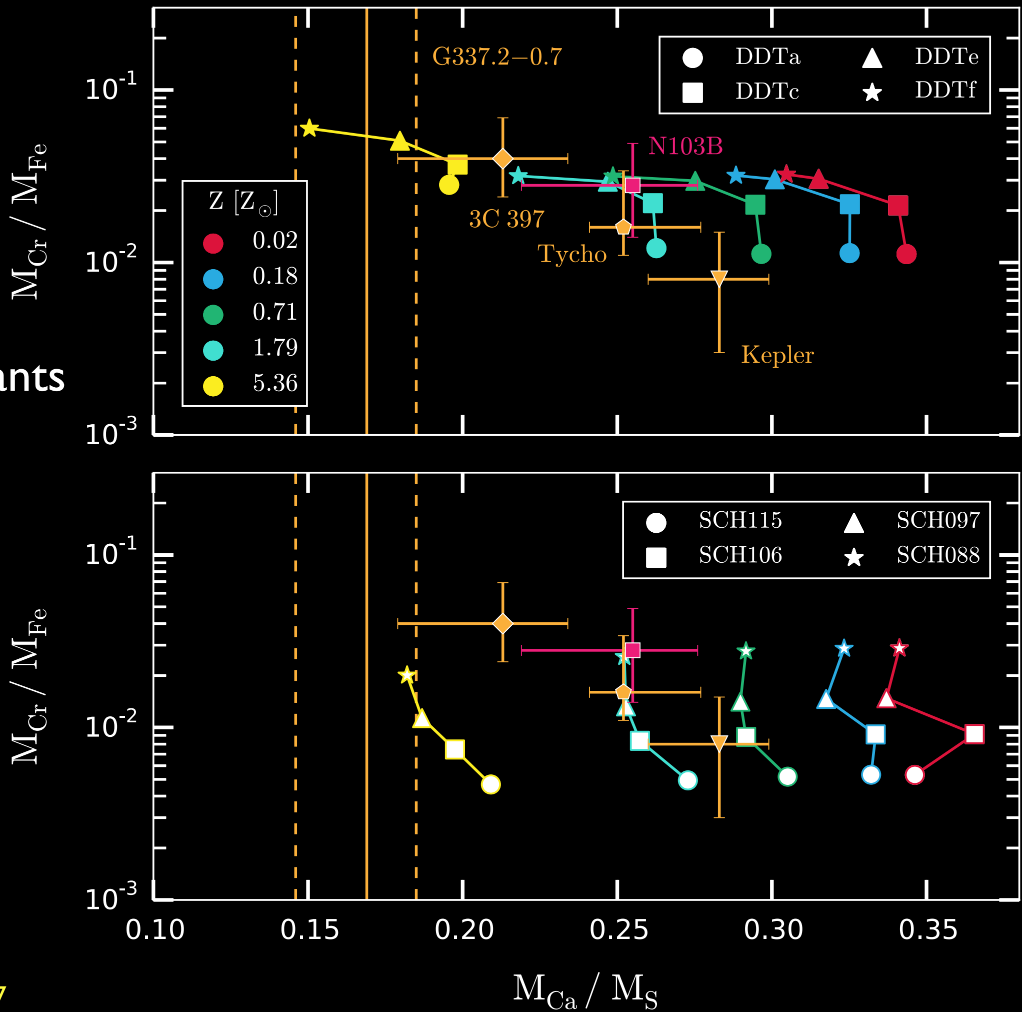

Martínez-Rodríguez et al 2017

Ca and Fe features at 4200 Å and 5200 Å at 30 days after explosion appear to deepen with progenitor metallicity.

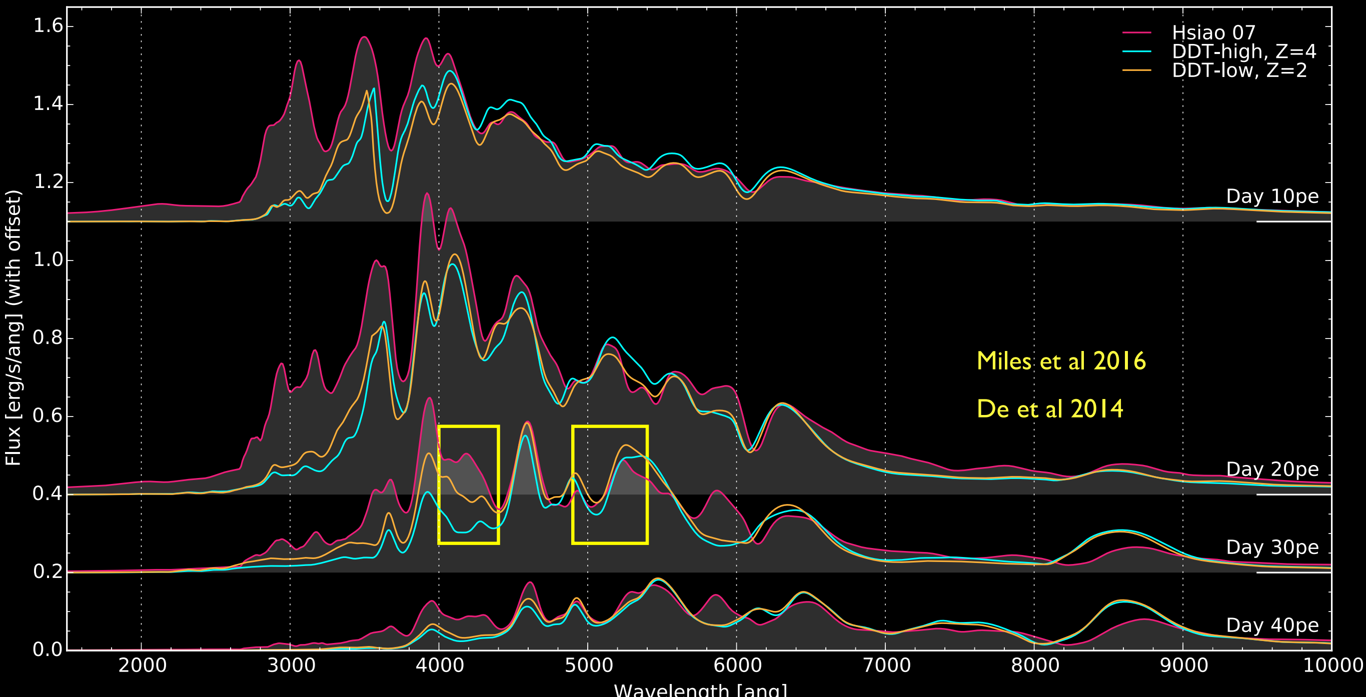

These features may allow for differentiation among progenitor metallicities and potentially help reduce the intrinsic Hubble scatter.

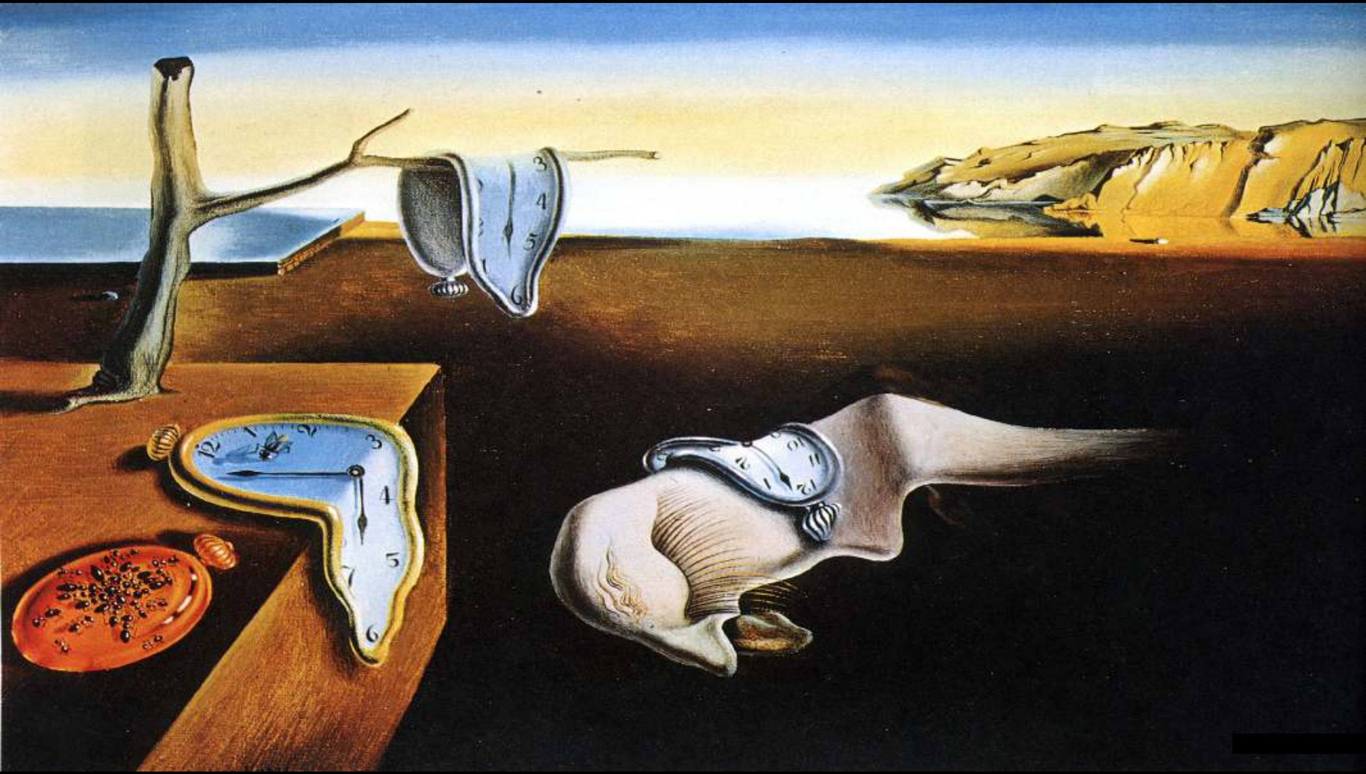

Dali, 1931
Oil on canvas
24 cm × 33 cm
MOMA NYC

3D Element Factories

Astronomy texts stress that massive stars are element factories that produce most of the periodic table of the elements.

Yet, our most advanced 3D supernova explosion simulations rely on ~21 isotopes to predict the energy generation and nucleosynthesis.

This yawning gap between element factories and 21 isotopes in 3D simulations is due, in part, by choosing to invest increasing compute capabilities into spatial resolution rather than the number of isotopes.

100 isotopes project

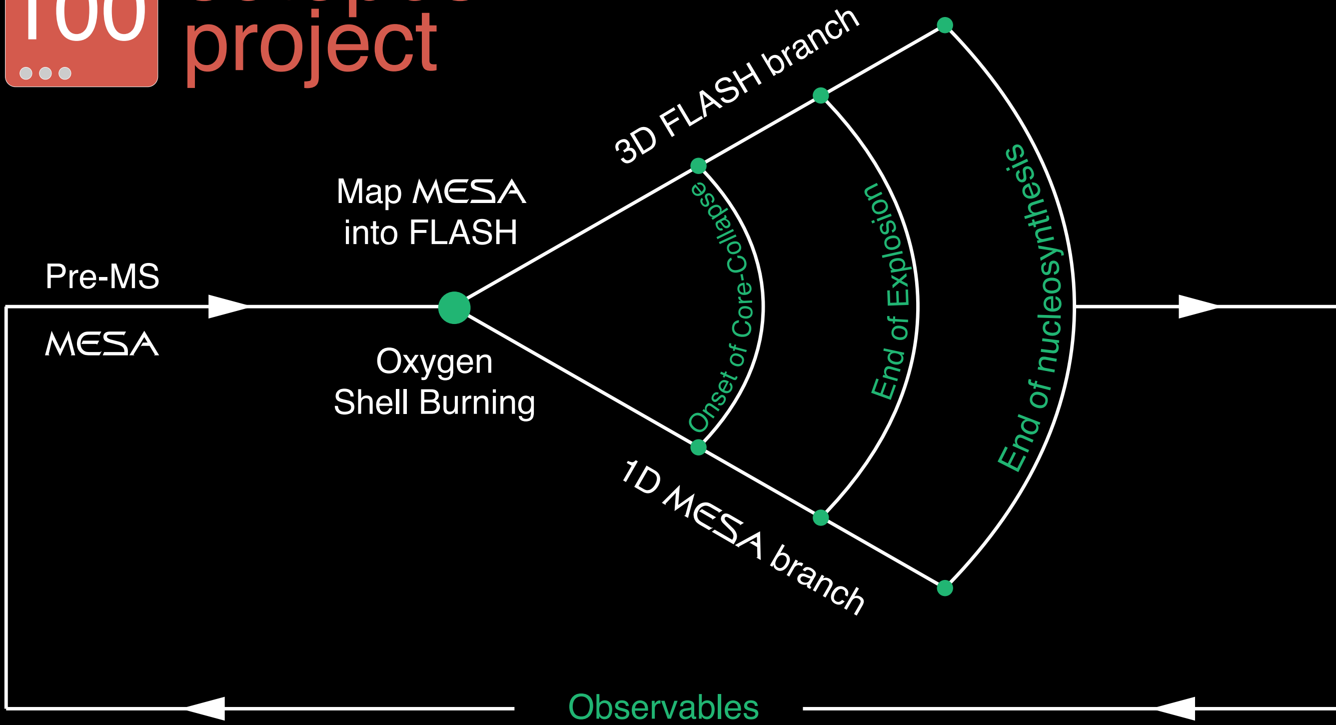

Radioactivities:
^{56}Ni, ^{57}Ni, ^{60}Fe, ^{55}Fe
^{56}Co, ^{57}Co, ^{60}Co, ^{44}Ti
^{26}Al

Stable Isotopes:
Fe, Si, O, C

Objects:
Cas A, SN87A

Timmes & Couch 2016

Beyond carbon burning, a minimum of ≈130 isotopes is needed for convergence of Y_e and the locations of the burning shells at the ≈10% level.

This 21 isotope MESA model was mapped into a 21 isotope 3D FLASH initial model during shell Si-burning.

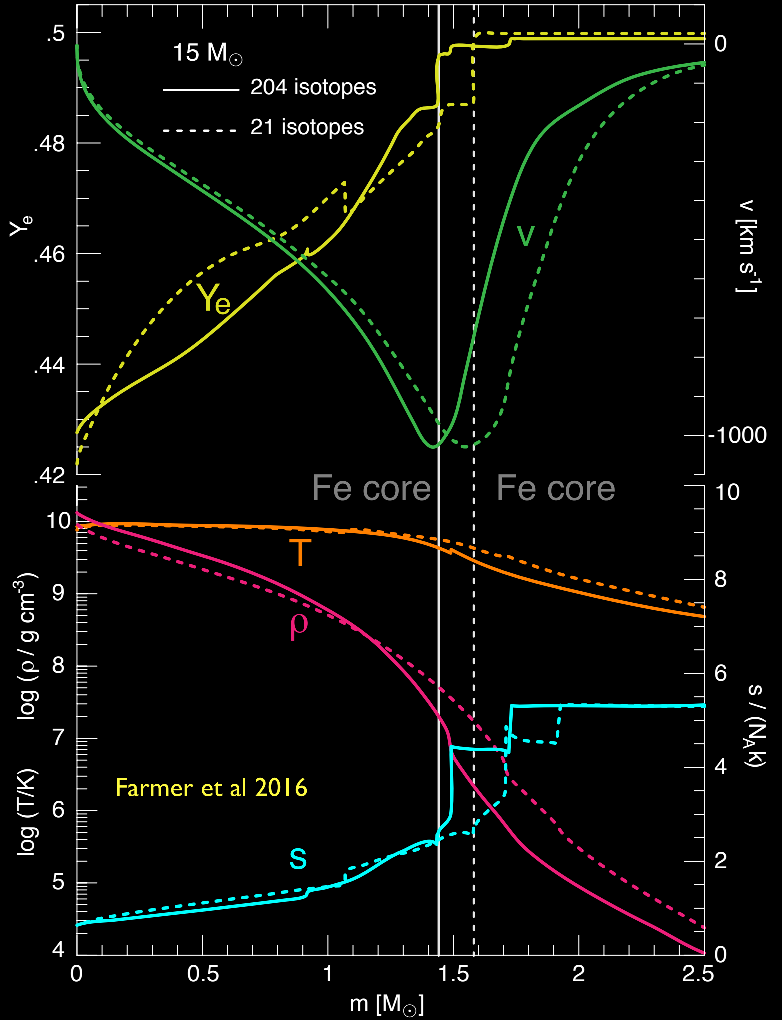

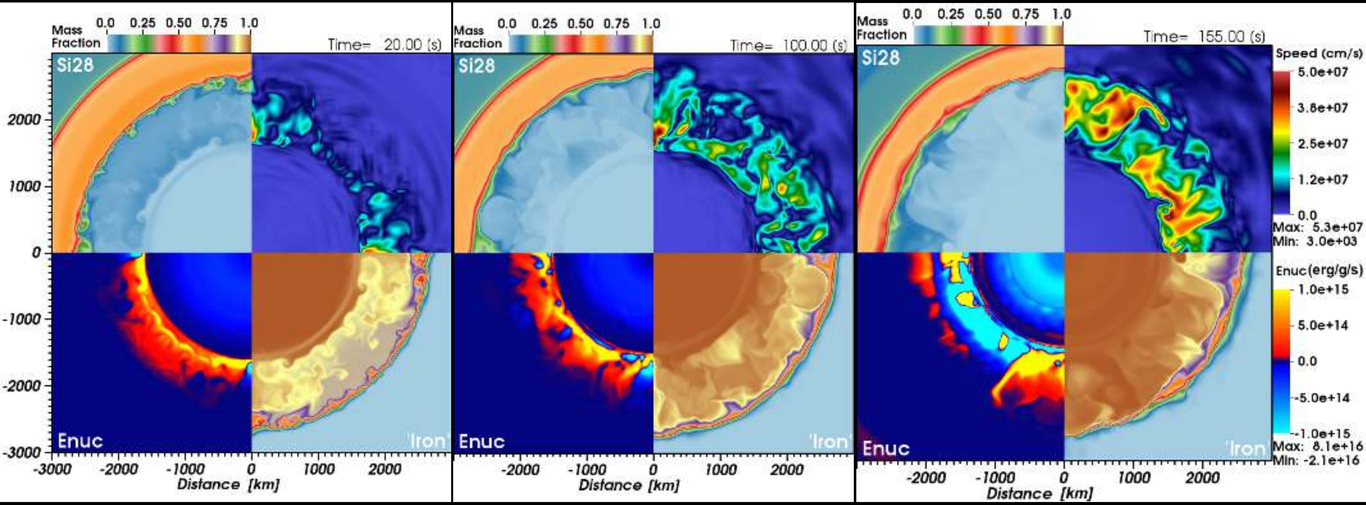

Couch et al 2015

First 3D simulation of the final minutes of iron core growth in a massive star, up to and including core-collapse.

A non-spherical progenitor has a significant impact on the likelihood for explosion, enhancing the explosion energy.

Final Fe core masses are similar, correlated with the time it takes to reach collapse:

1.51 $M_\odot$ - fiducial MESA

1.46 $M_\odot$ - enhanced-rate MESA

1.50 $M_\odot$ - 3D FLASH simulation.

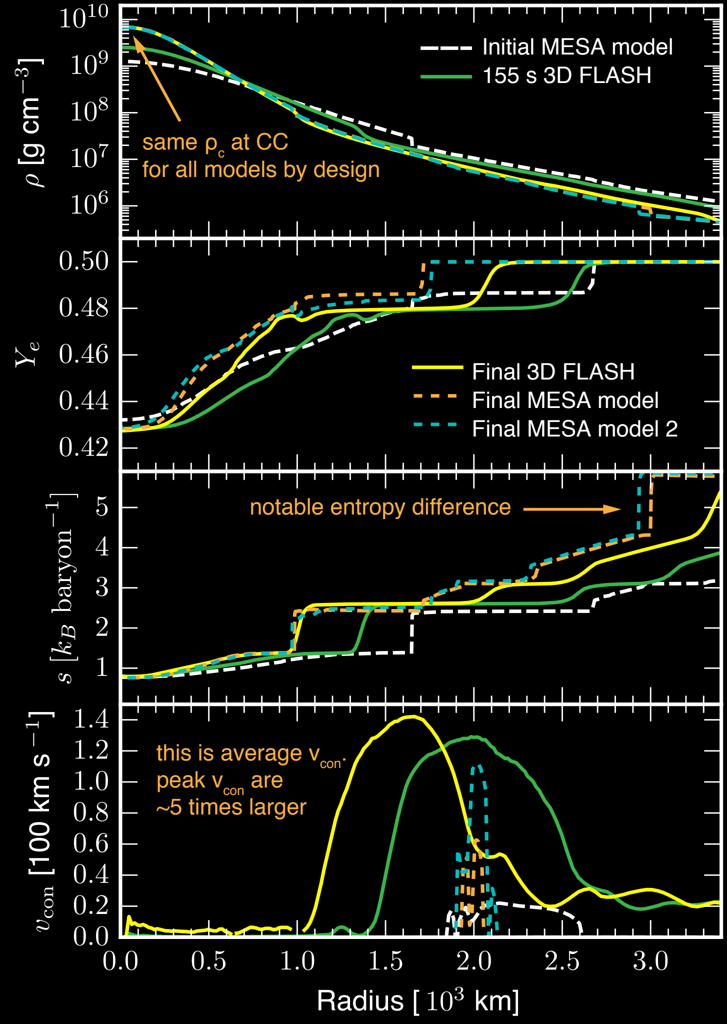

Caution: more exploration is needed to assess the fidelity of 1D structure to 3D physics.

The stronger turbulence excited by 3D initial conditions gives a greater (diagnostic) explosion energy.

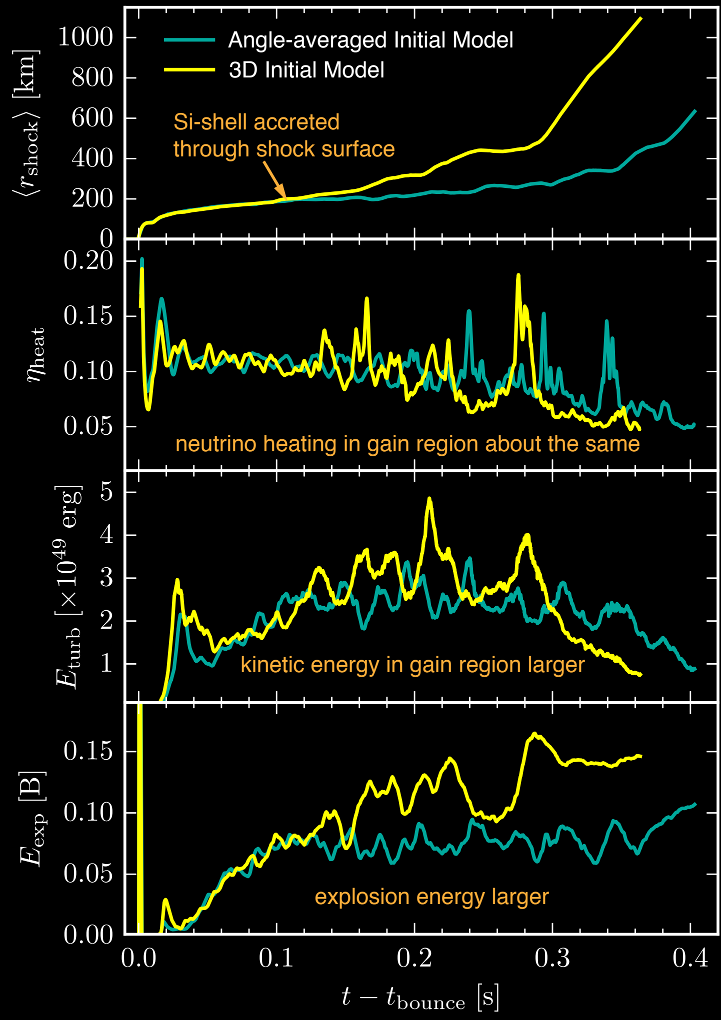

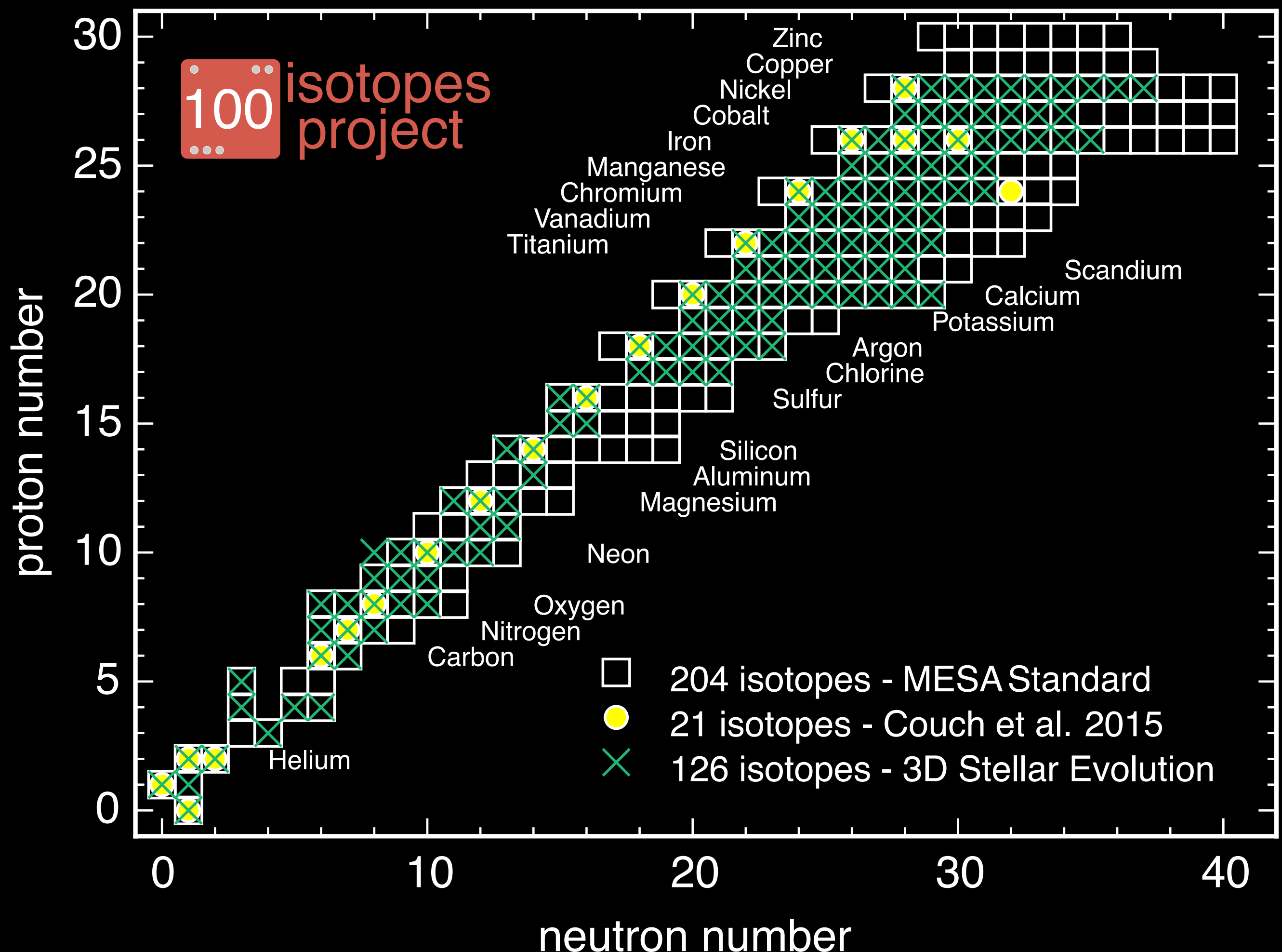

100 isotopes project
proton number
neutron number
0
5
10
15
20
25
30
0
10
20
30
40
Zinc
Copper
Nickel
Cobalt
Iron
Manganese
Chromium
Vanadium
Titanium
Scandium
Calcium
Potassium
Argon
Chlorine
Sulfur
Silicon
Aluminum
Magnesium
Neon
Oxygen
Nitrogen
Carbon
Helium
204 isotopes - MESA Standard
21 isotopes - Couch et al. 2015
126 isotopes - 3D Stellar Evolution

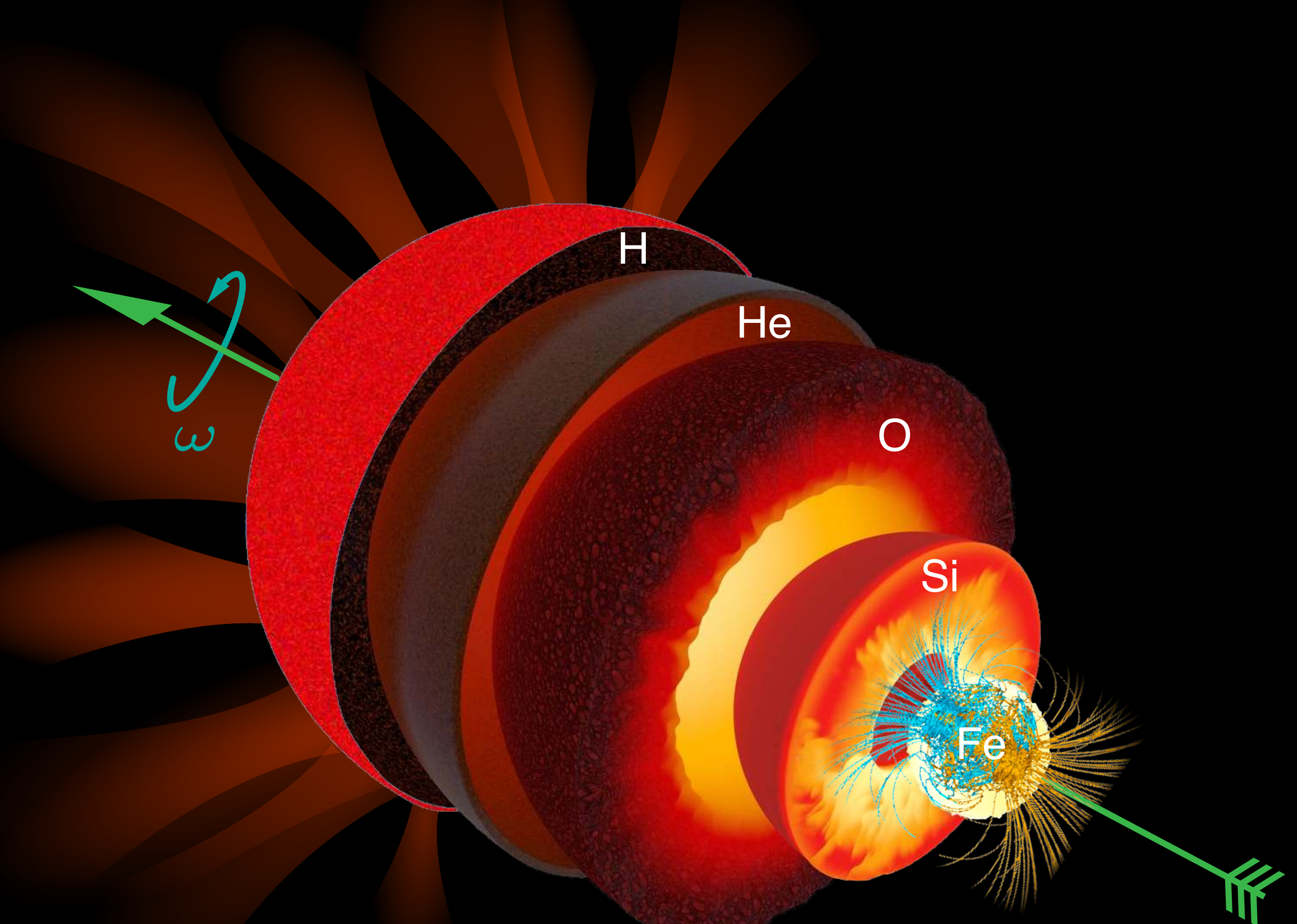

“getting the progenitor right”

26 Modes of Uncertainty

Stars are gravitationally confined thermonuclear reactors.

How do the properties of CO white dwarfs, evolved from the main-sequence, vary with respect to the composite uncertainties in the reaction rates?

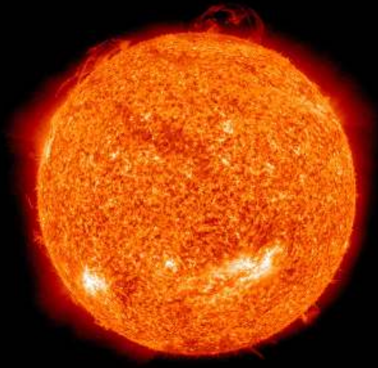

$\sum \delta(\text{reaction rates}) = ?$

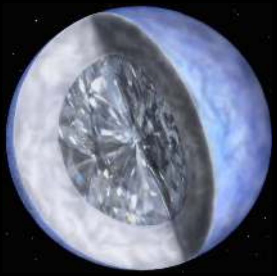

STARLIB is the first (and only) reaction rate library that gives a Monte Carlo / Bayesian reaction rate probability density for a reaction due to experimental uncertainties.

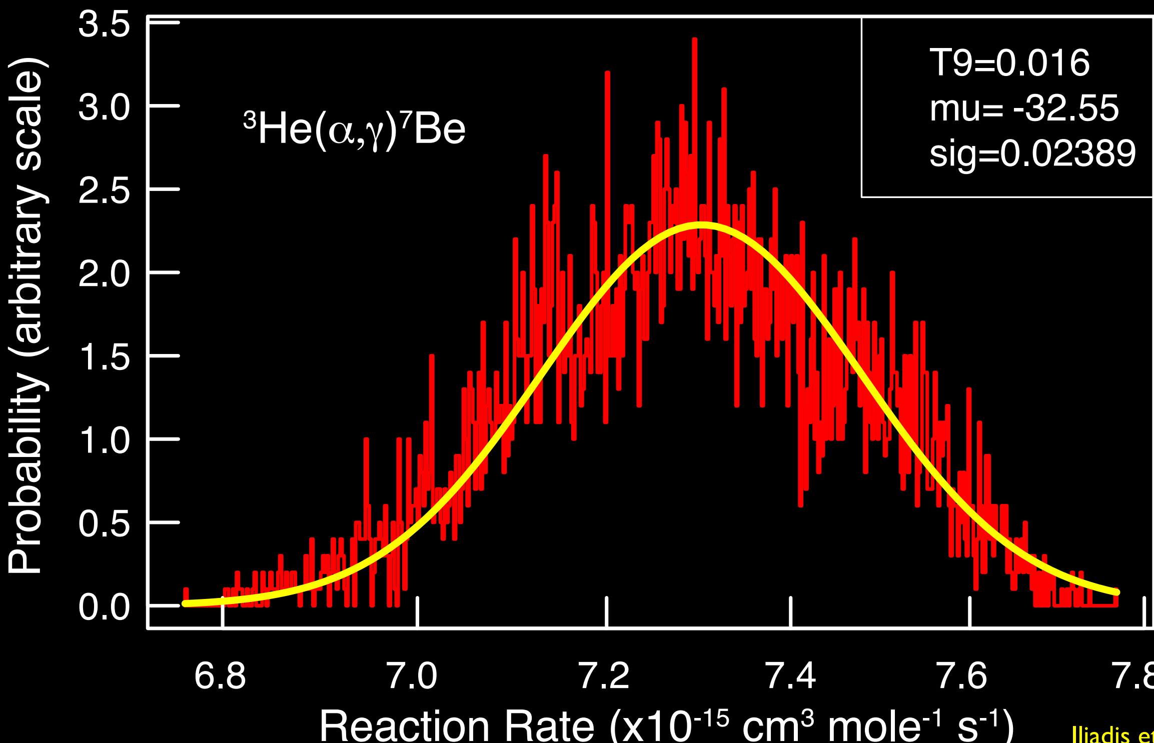

Iliadis et al 2016

First Monte Carlo stellar evolution study of a 3 $M_\odot$ model evolved from the pre main-sequence to a white dwarf.

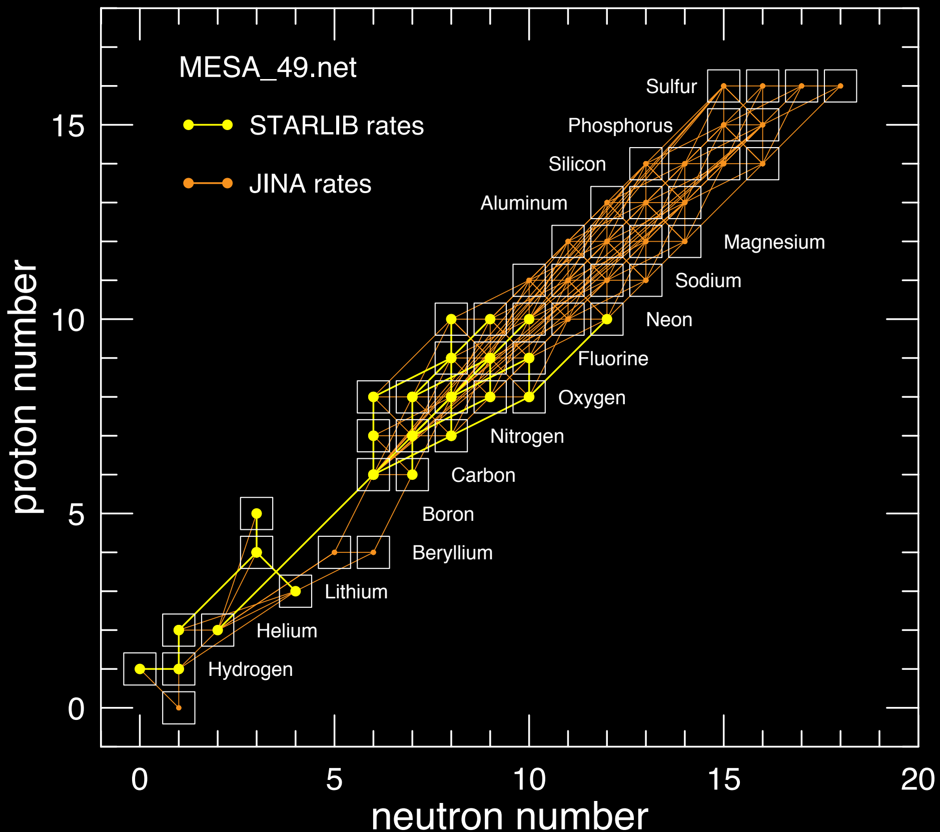

Fields et al 2016

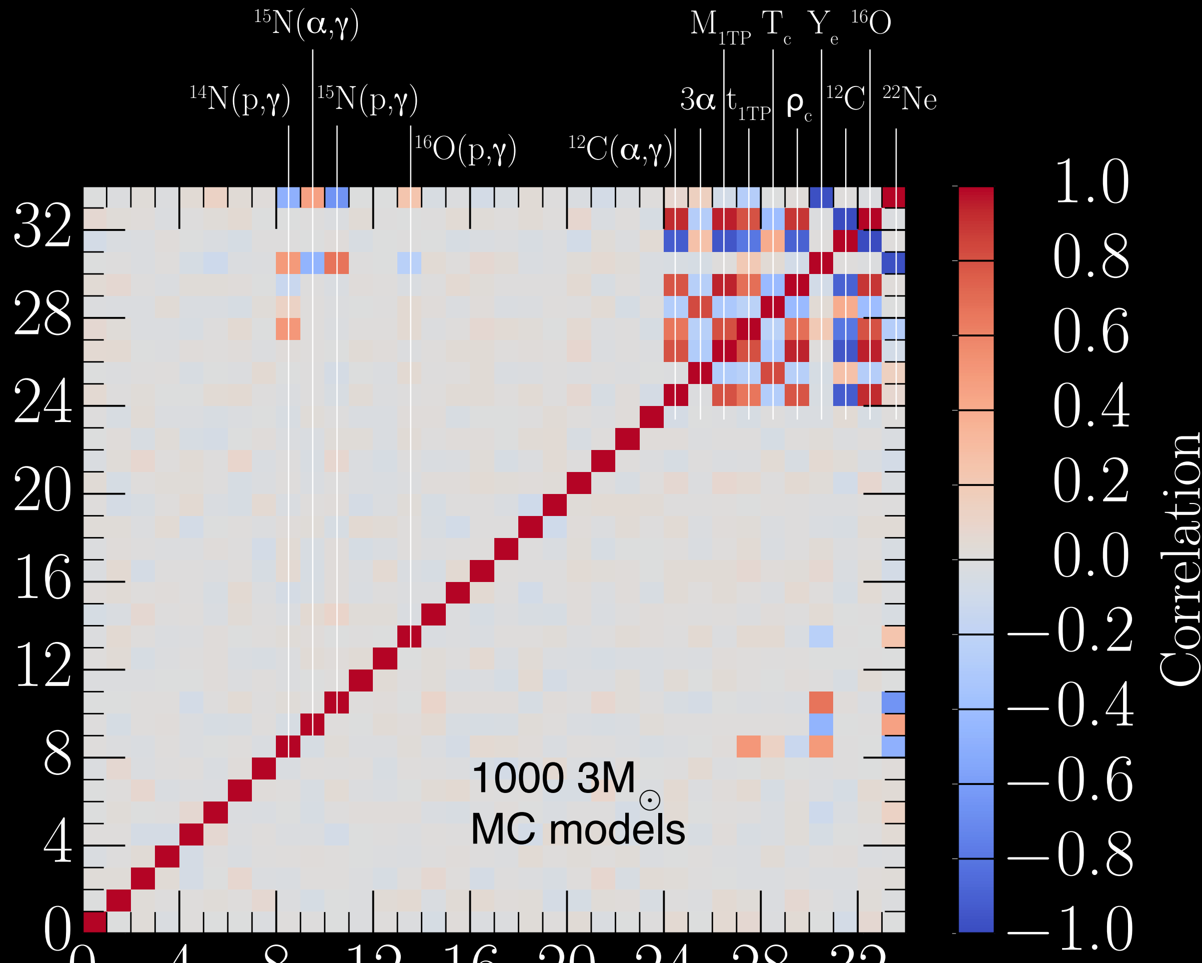

Fields et al 2016

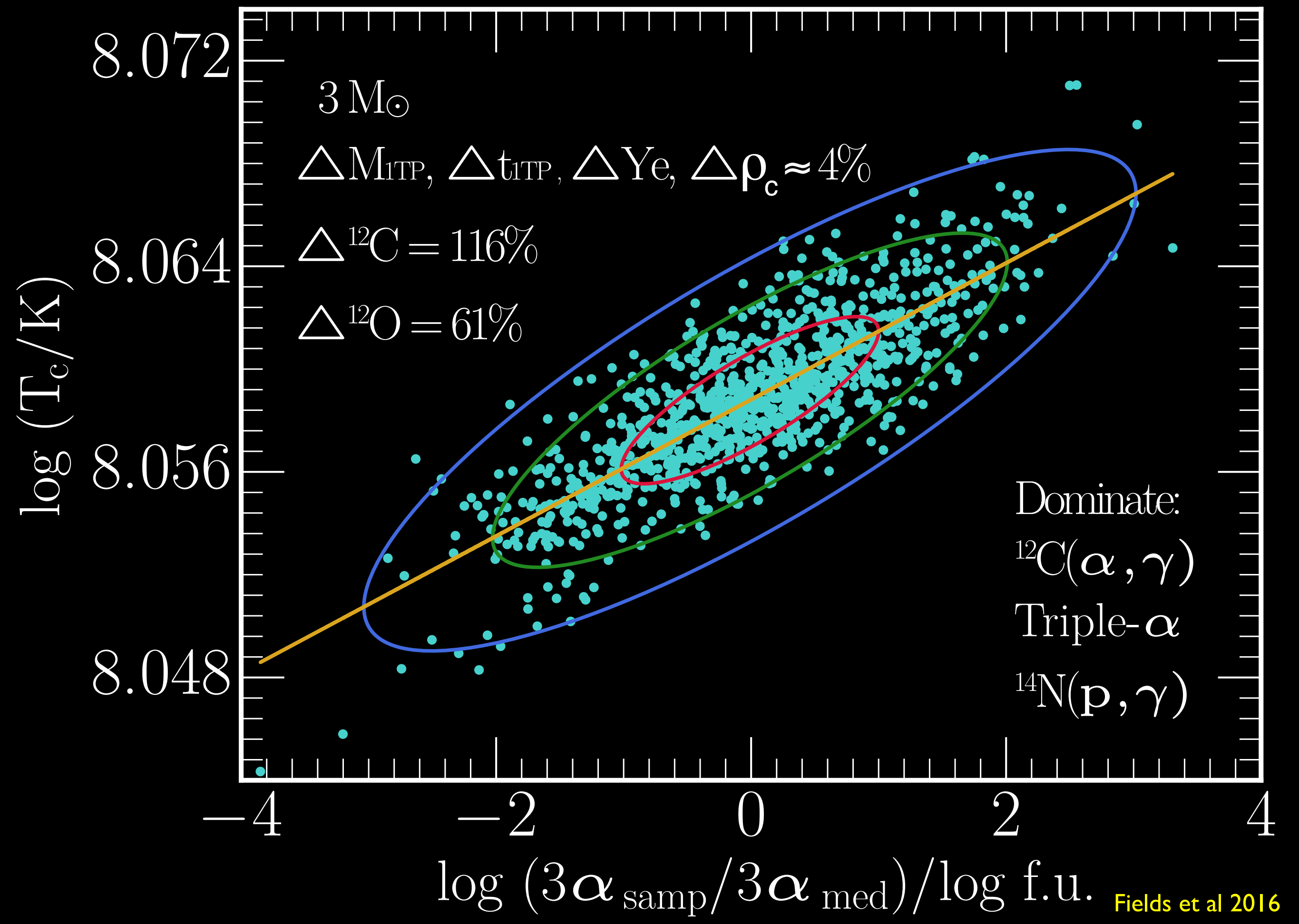
3 M⊙
△M1TP, △t1TP, △Ye, △ρc ≈ 4%
△12C = 116%
△12O = 61%
Dominate:
12C(α, γ)
Triple-α
14N(p, γ)
8.072
8.064
8.056
8.048
log (Tc/K)
−4
−2
0
2
4
log (3α samp/3α med)/log f.u.
Fields et al 2016

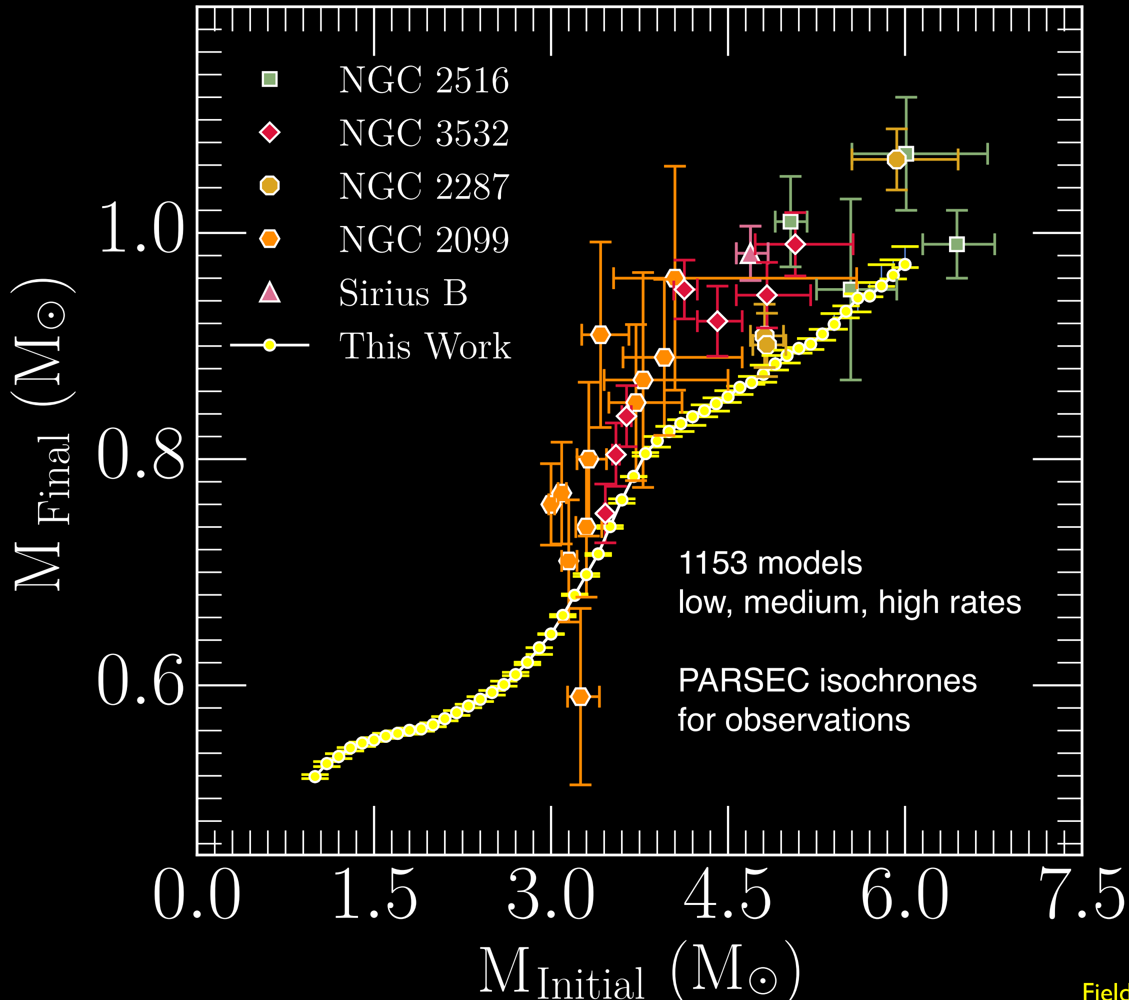

Fields et al 2016

The Short and Long of Paper Citations

Are the papers that drive the AAS journals impact factor (a 2 year horizon) the same papers that the community values 5 years later? 10 years later? 20 years?

Is MNRAS eating the AAS's lunch?

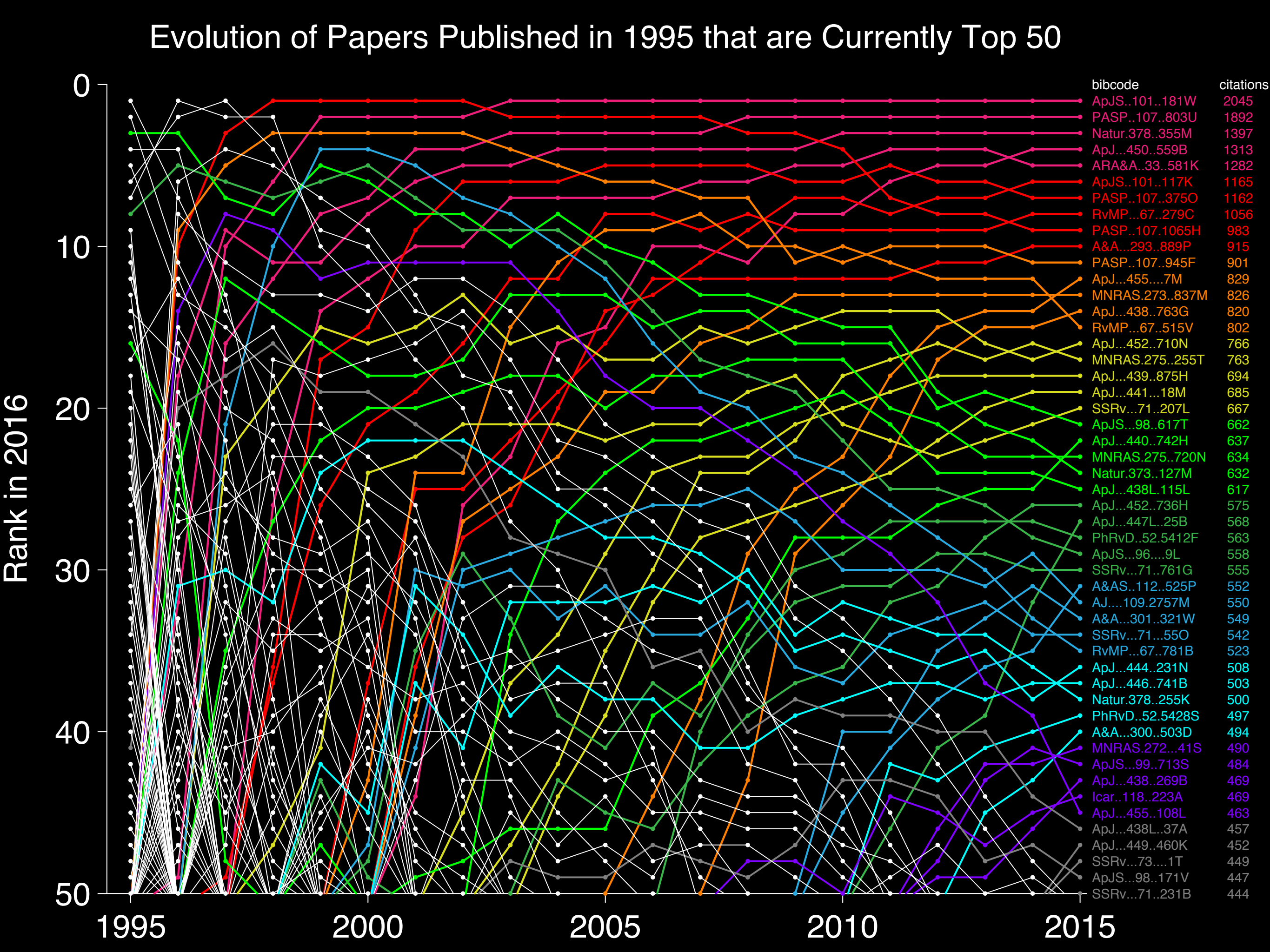
Evolution of Papers Published in 1995 that are Currently Top 50
Rank in 2016
0
10
20
30
40
50
1995
2000
2005
2010
2015
bibcode citations
ApJS..101..181W 2045
PASP..107..803U 1892
Natur.378..355M 1397
ApJ...450..559B 1313
ARA&A..33..581K 1282
ApJS..101..117K 1165
PASP..107..375O 1162
RvMP...67..279C 1056
PASP..107.1065H 983
A&A...293..889P 915
PASP..107..945F 901
ApJ...455....7M 829
MNRAS.273..837M 826
ApJ...438..763G 820
RvMP...67..515V 802
ApJ...452..710N 766
MNRAS.275..255T 763
ApJ...439..875H 694
ApJ...441...18M 685
SSRv...71..207L 667
ApJS...98..617T 662
ApJ...440..742H 637
MNRAS.275..720N 634
Natur.373..127M 632
ApJ...438L.115L 617
ApJ...452..736H 575
ApJ...447L..25B 568
PhRvD..52.5412F 563
ApJS...96....9L 558
SSRv...71..761G 555
A&AS..112..525P 552
AJ....109.2757M 550
A&A...301..321W 549
SSRv...71...55O 542
RvMP...67..781B 523
ApJ...444..231N 508
ApJ...446..741B 503
Natur.378..255K 500
PhRvD..52.5428S 497
A&A...300..503D 494
MNRAS.272...41S 490
ApJS...99..713S 484
ApJ...438..269B 469
Icar..118..223A 469
ApJ...455..108L 463
ApJ...438L..37A 457
ApJ...449..460K 452
SSRv...73....1T 449
ApJS...98..171V 447
SSRv...71..231B 444

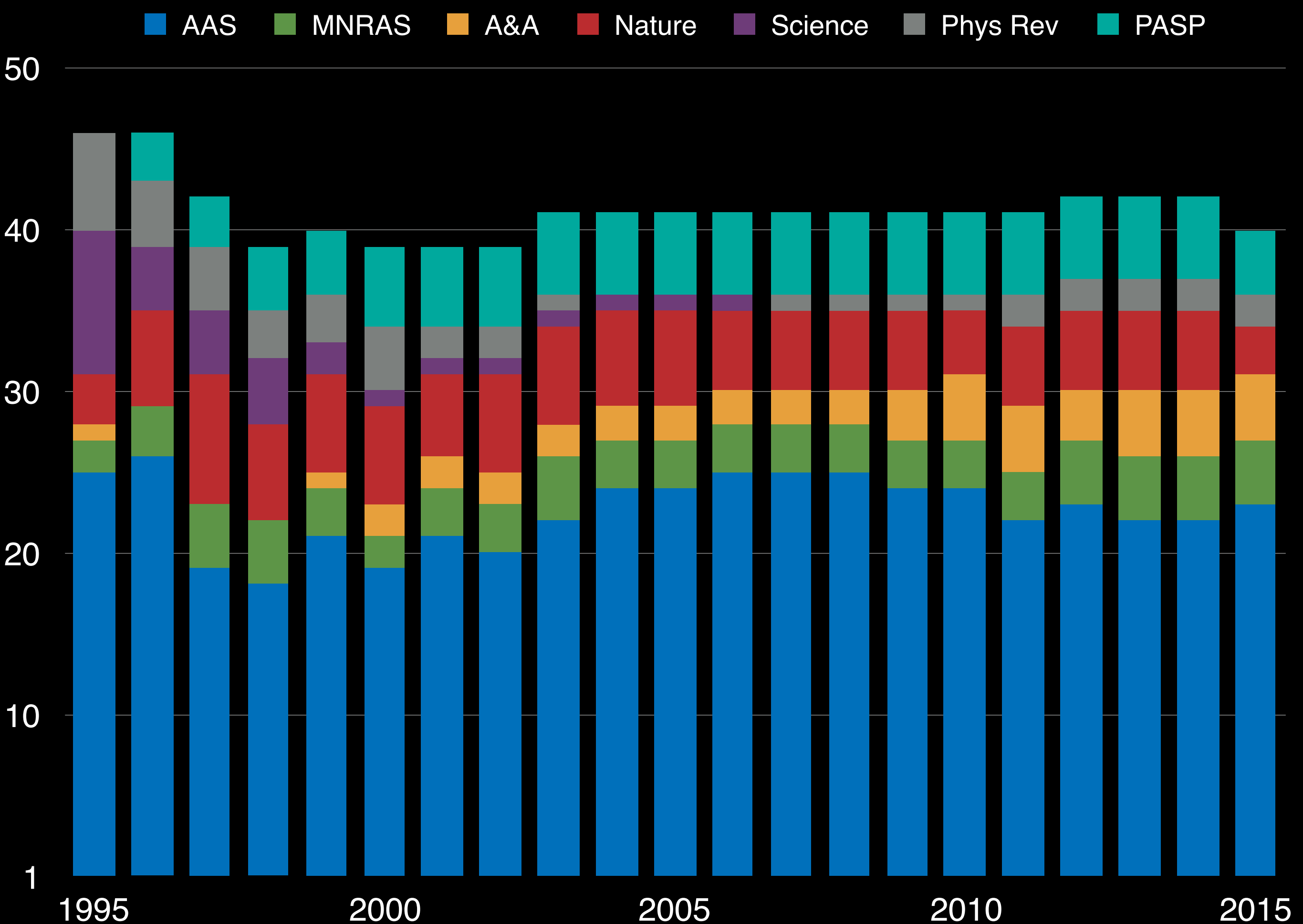
AAS
MNRAS
A&A
Nature
Science
Phys Rev
PASP
50
40
30
20
10
1
1995
2000
2005
2010
2015

Astrolabe

Illuminating Astronomy Data

Observed correlations between the peak luminosity and width of the light curve help in the hunt for the progenitors.

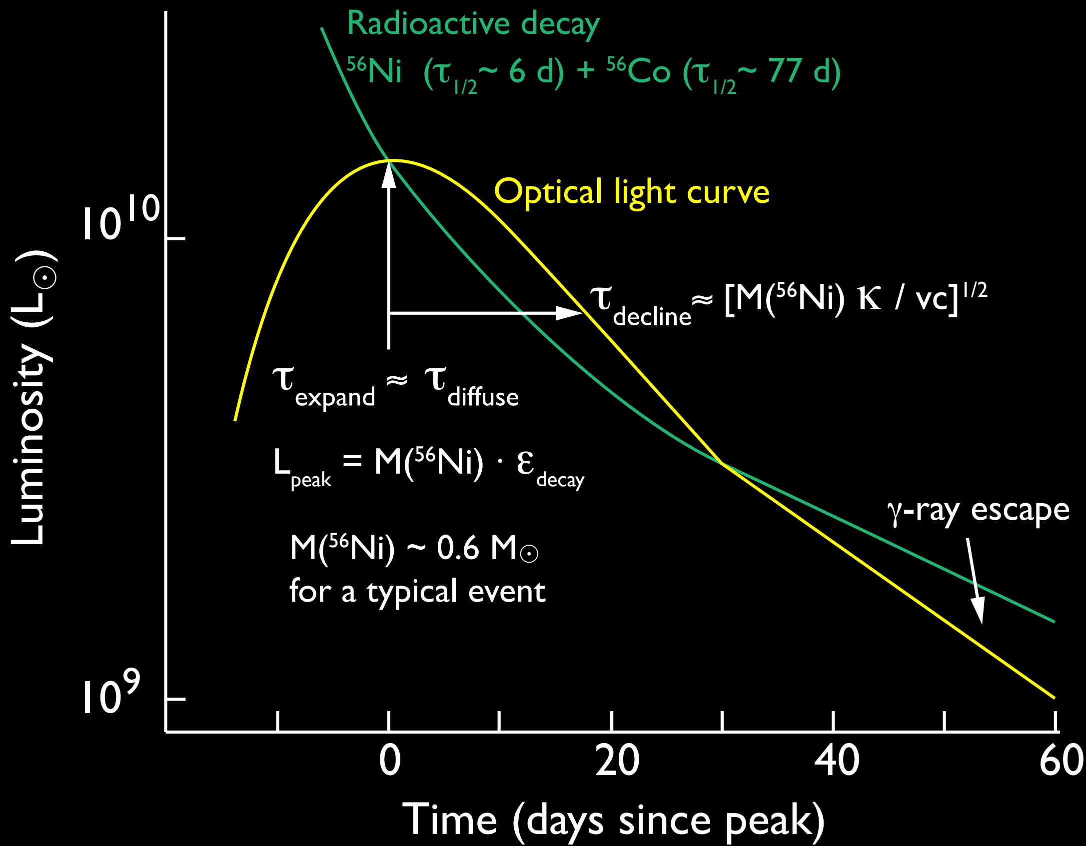

Smashing White Dwarfs

Single-Degenerate channel

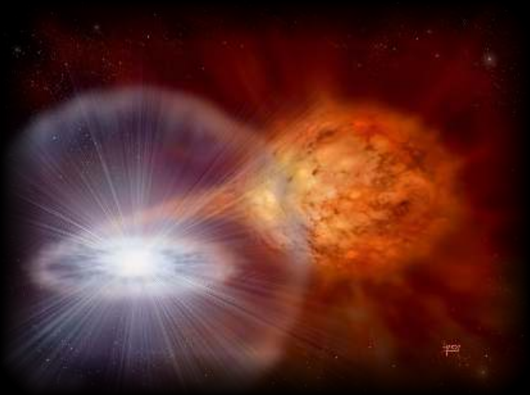

Double-Degenerate channel

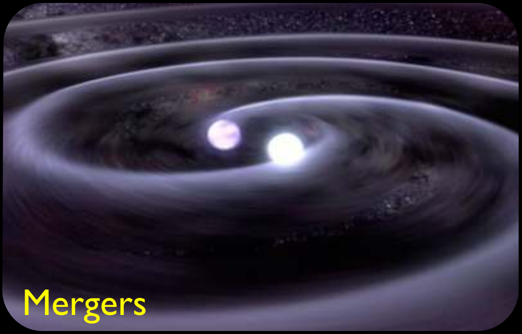

The relative frequency of these channels is unknown.

The first white dwarf smashes were calculated in 1985:

3D, 5000 particles with nuclear burning done afterwards and approximate thermodynamics.

Bottom line:
Tiny amounts of ^{56}Ni produced.

Message:
Nothing here, move along.

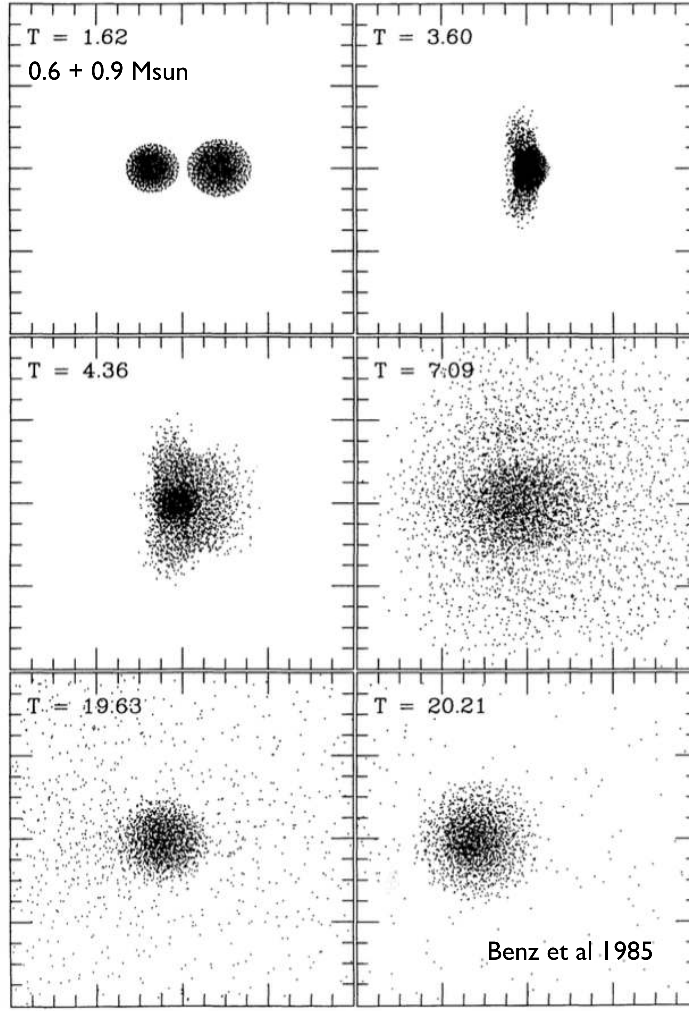

2010: 2 million particles with inline burning and realistic thermodynamics.

0.6 + 0.6 $M_{\odot}$, zero impact parameter, x-y plane, temperature.

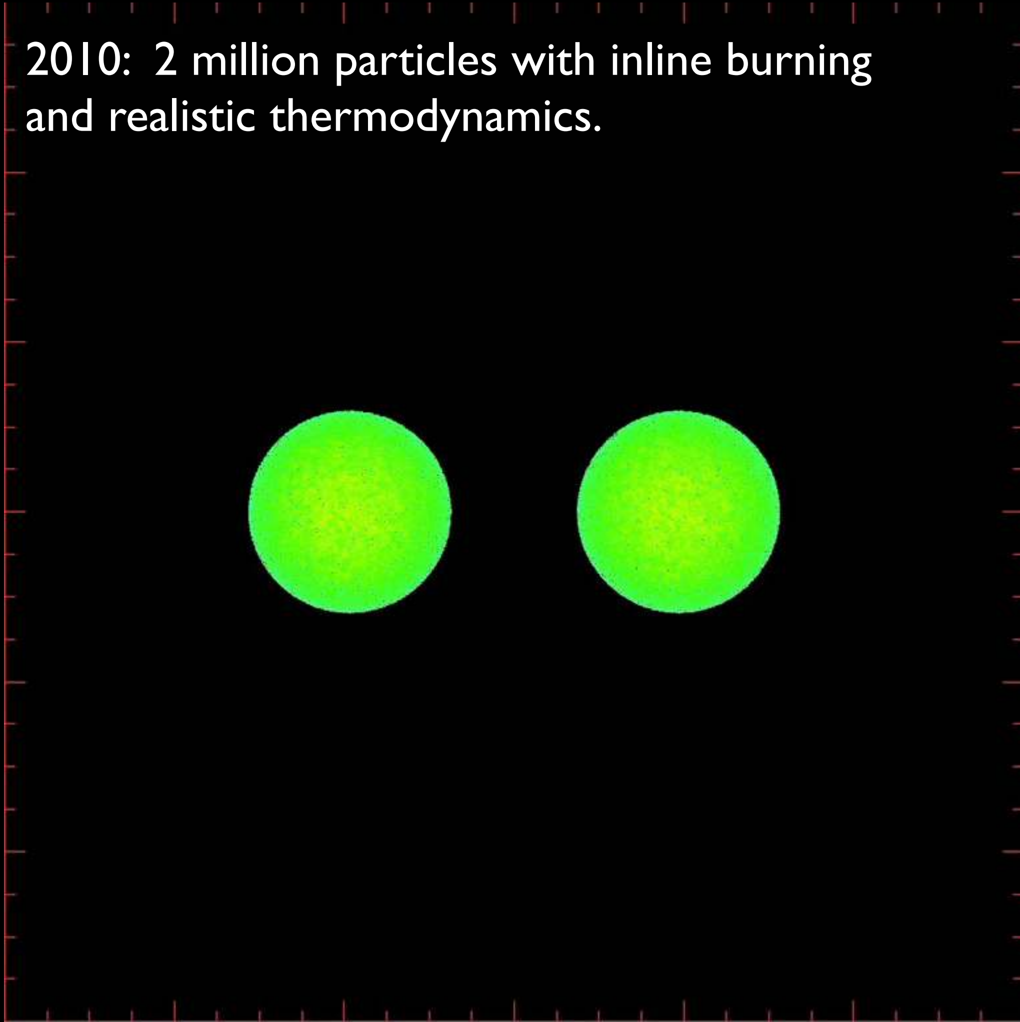

Raskin et al 2010

Message in 2010: Lots of interesting possibilities!

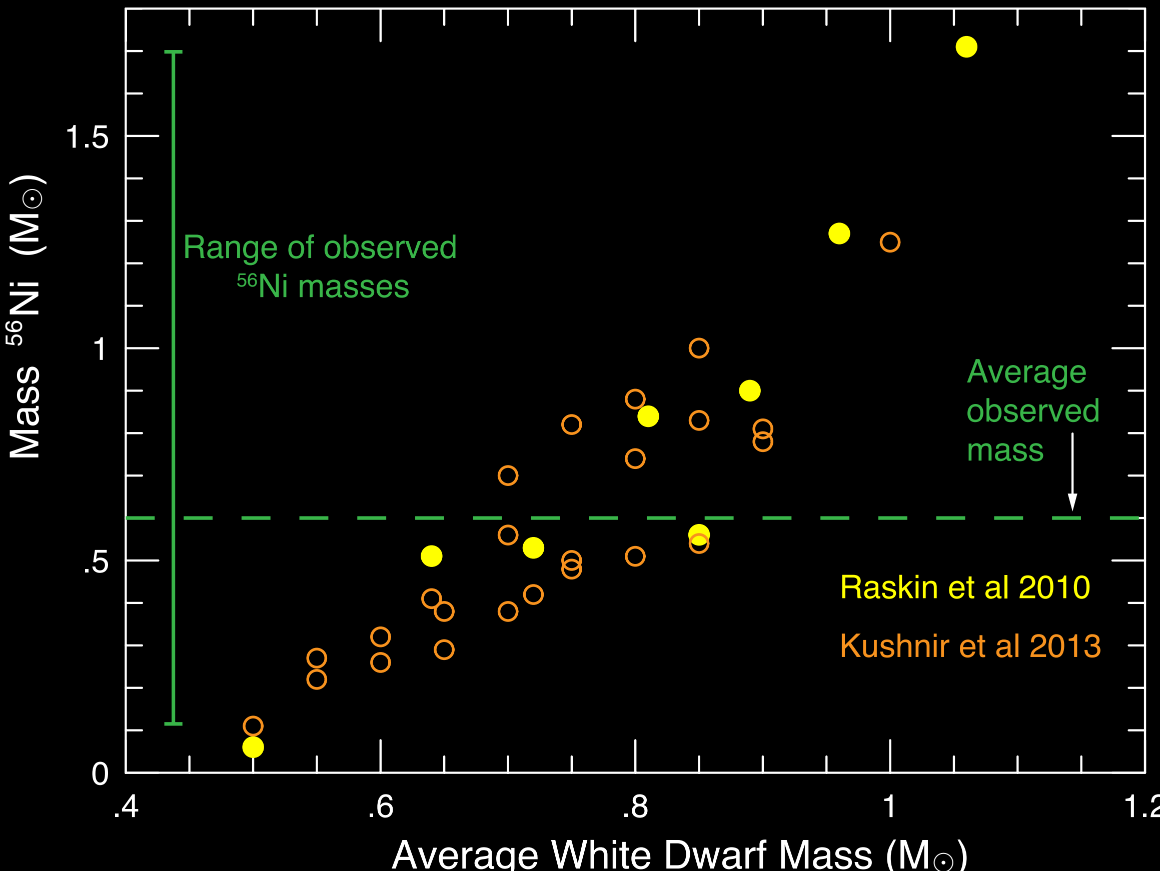

Observations suggest about 5 million white dwarf supernova per year within a redshift of one.

An objection to the collision scenario is the perception that they are extremely rare.

Duel Between Onegin and Lenski

Ilya Repin (1899)

Pen, brush, ink, watercolor.

Pushkin Museum, Moscow

Collisions have been believed to predominantly occur in dense stellar environments, such as cores of globular clusters.

Even accounting for gravitational focusing, the collision rate is ~5000 per year within a redshift of one.

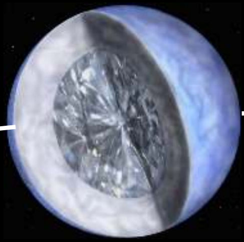

$$\sigma = \pi b^2 = \pi R^2 \left[1 + \left(\frac{v_{\rm esc}}{v}\right)^2\right]$$

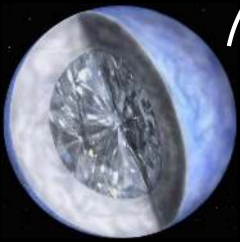

Like a duel, this mechanism is single shot.

Wait! There is a 3rd body in this duel.

Duel Between Onegin and Lenski

Ilya Repin (1899)

Pen, brush, ink, watercolor.

Pushkin Museum, Moscow

Hierarchical triple star systems with white dwarf binary orbital separations of 1-300 AU are known to exist.

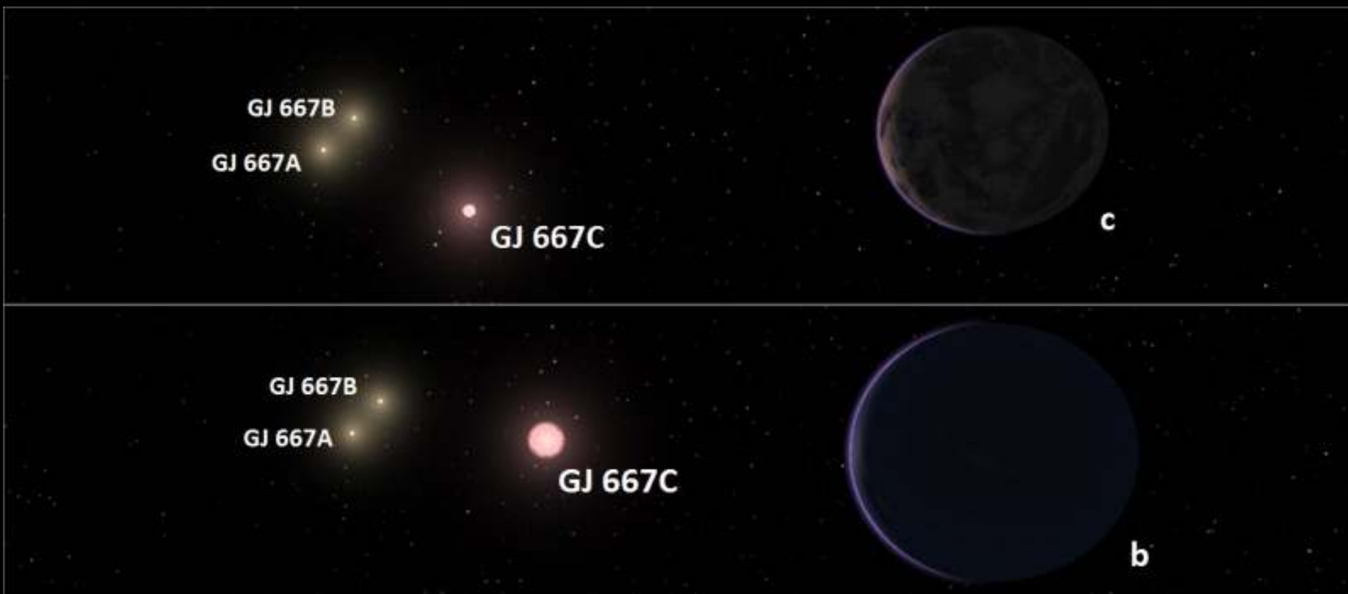

The white dwarf binary's ellipticity can be driven to large values in a triple star system because ellipticity can be traded for inclination in the conservation of angular momentum

$$L_z = \sqrt{1 - e^2}\ \cos(i)$$

in Kozai-Lidov oscillations.

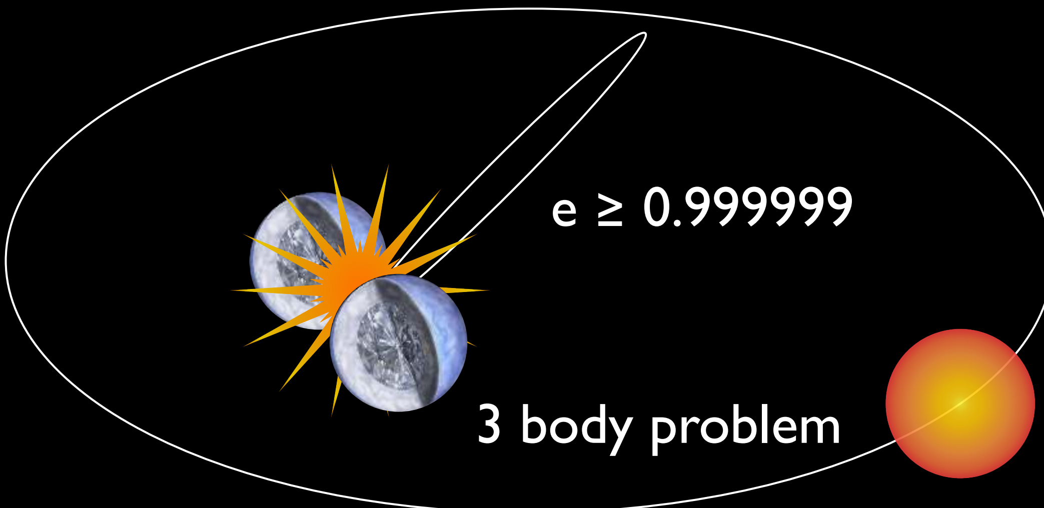

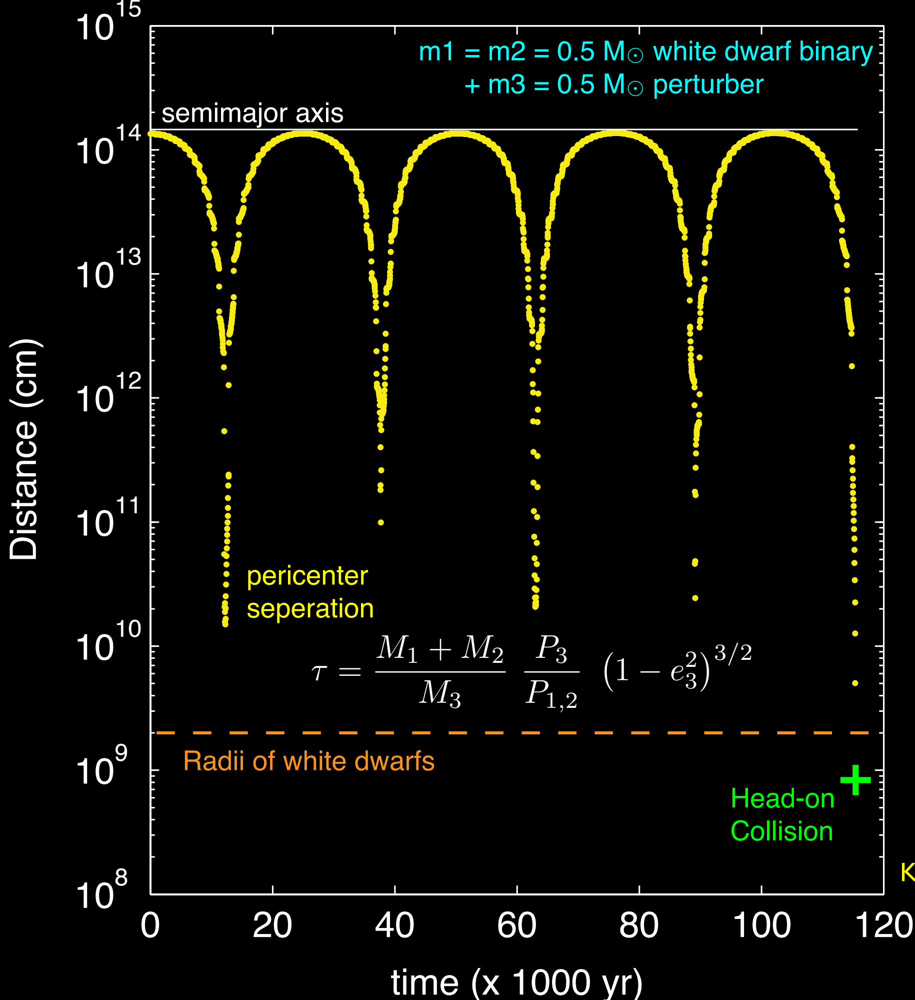

Katz & Dong 2010

White dwarfs in a triple star system have a ~3% chance of a head-on collision within 5 billion years.

Unlike a duel, this mechanism is repeated shots.

If 15-20 % of $1M_\odot \leq M \leq 8M_\odot$ stars have a $M > 1M_\odot$ companion, the collision scenario can dominate.

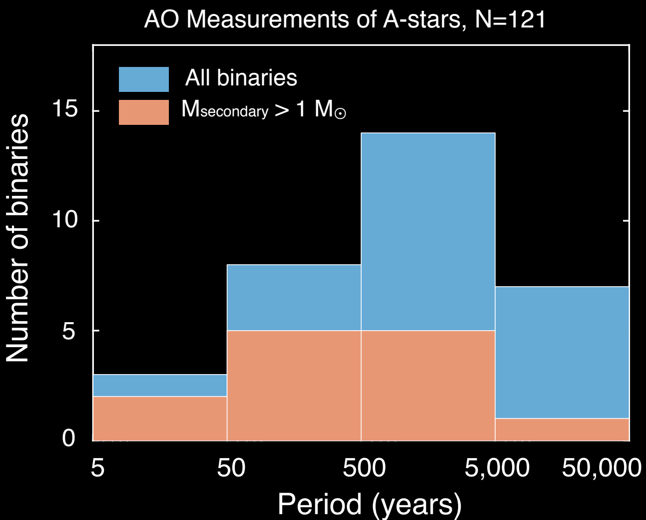

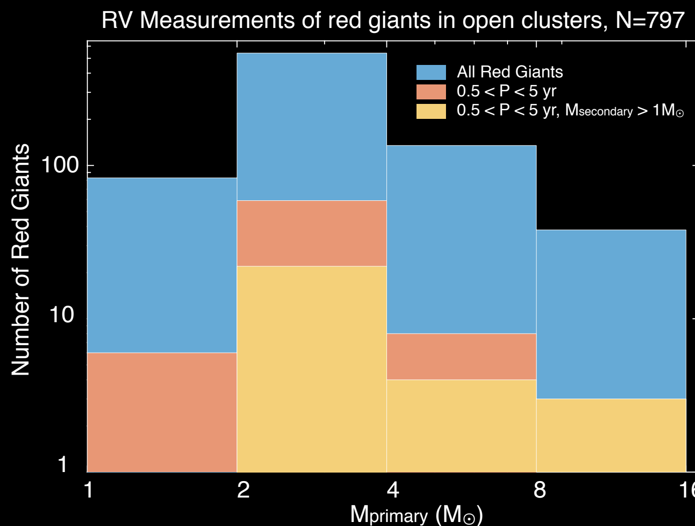

Klein & Katz 2017

Prediction: GAIA will find ~10 new wide orbit double degenerates within 20 pc from the Sun.

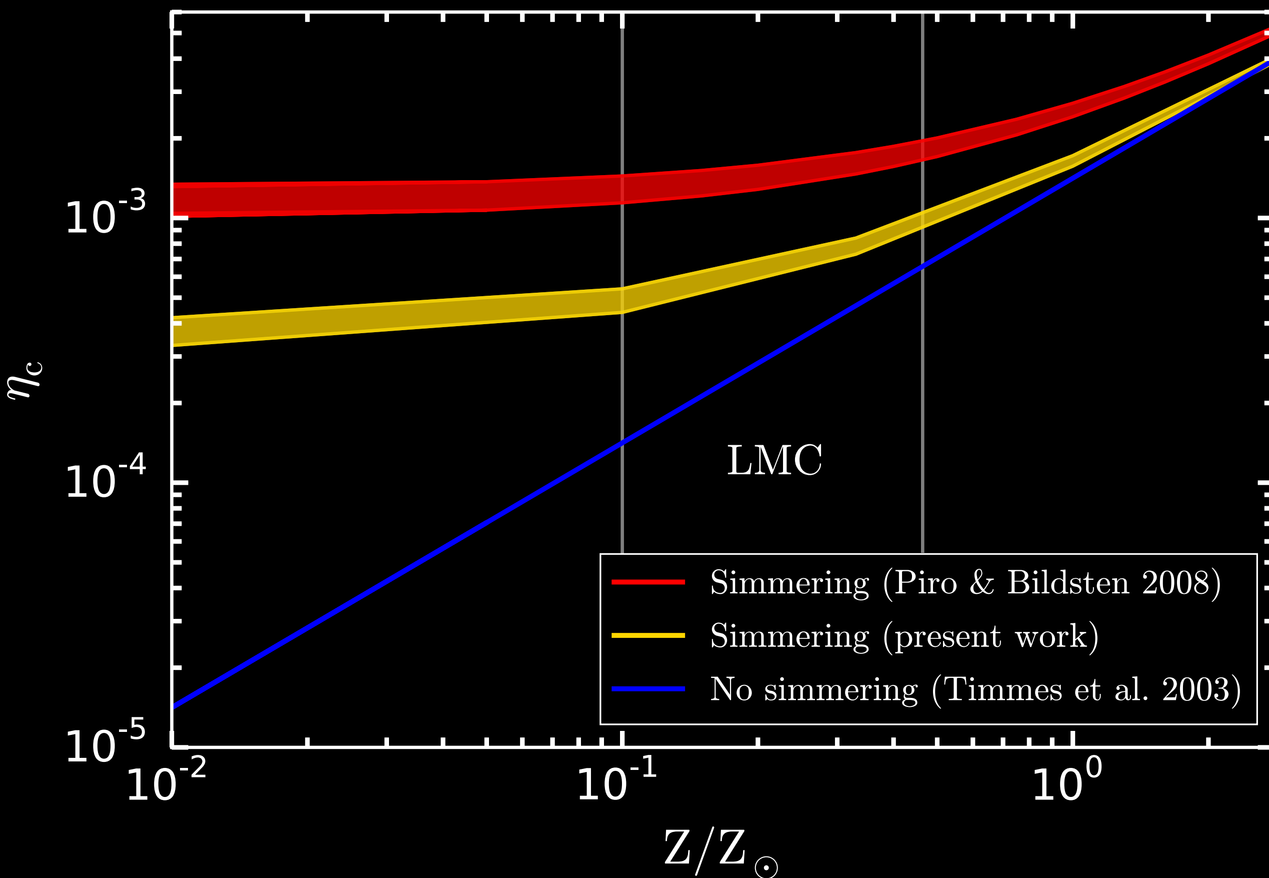

Martínez-Rodríguez et al 2016

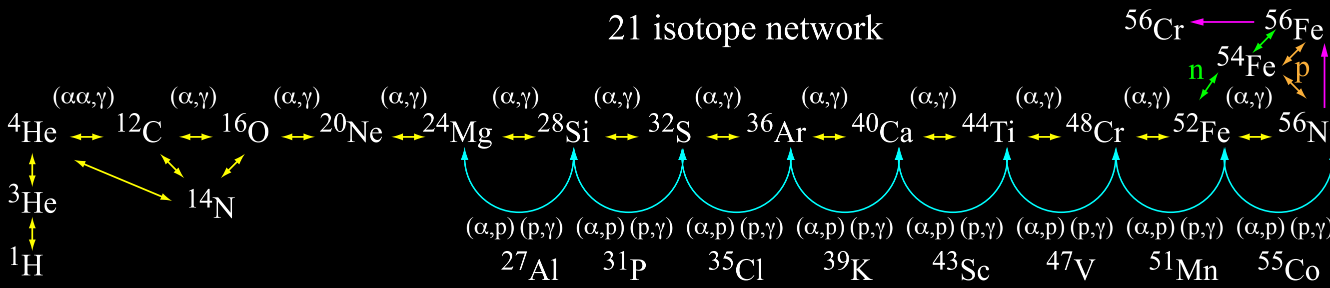

21 isotope network
4He
3He
1H
12C
14N
16O
20Ne
24Mg
28Si
32S
36Ar
40Ca
44Ti
48Cr
52Fe
56Ni
54Fe
56Fe
56Cr
n
p
(αα,γ)
(α,γ)
(α,p) (p,γ)
27Al
31P
35Cl
39K
43Sc
47V
51Mn
55Co

t = 15.92790

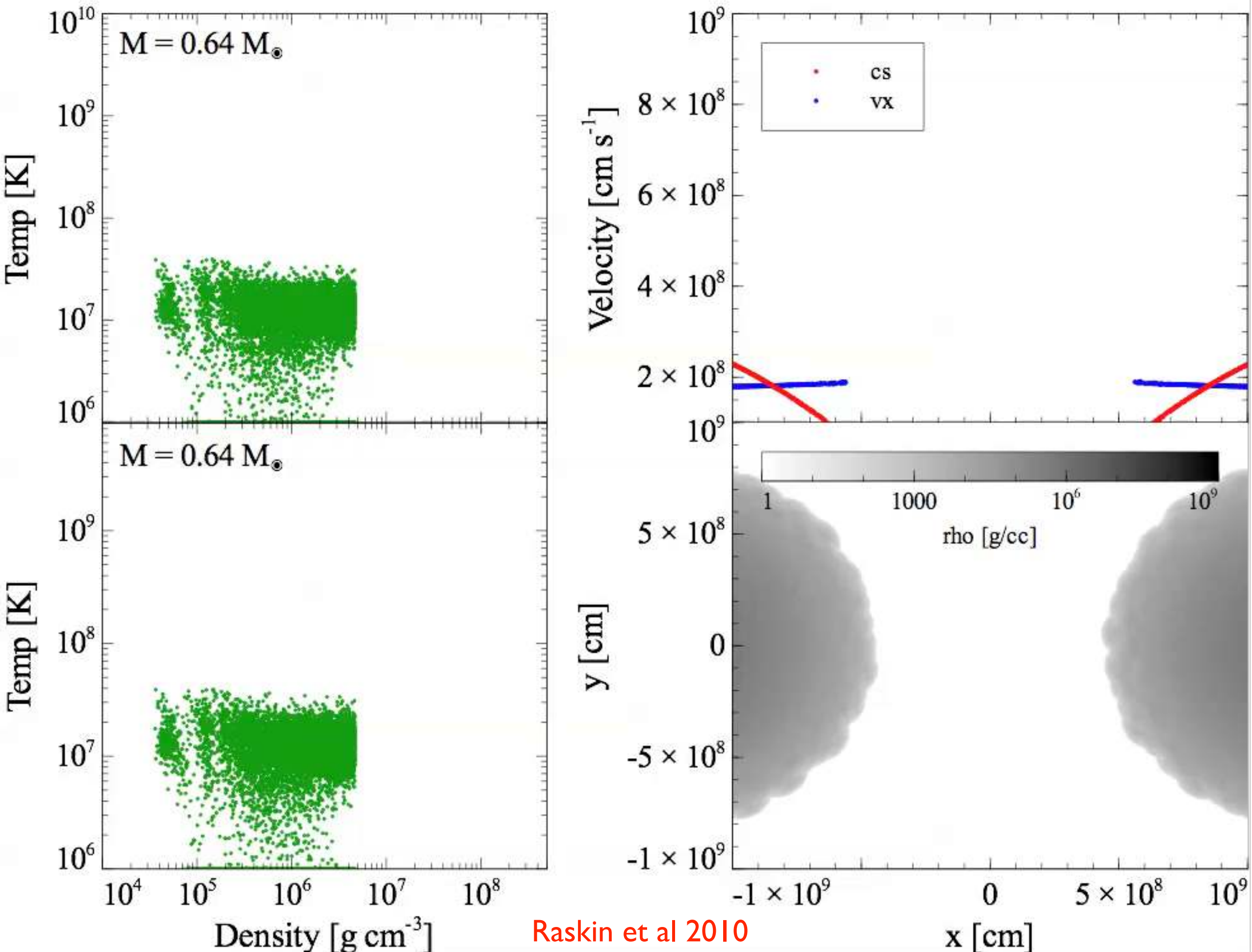

Raskin et al 2010

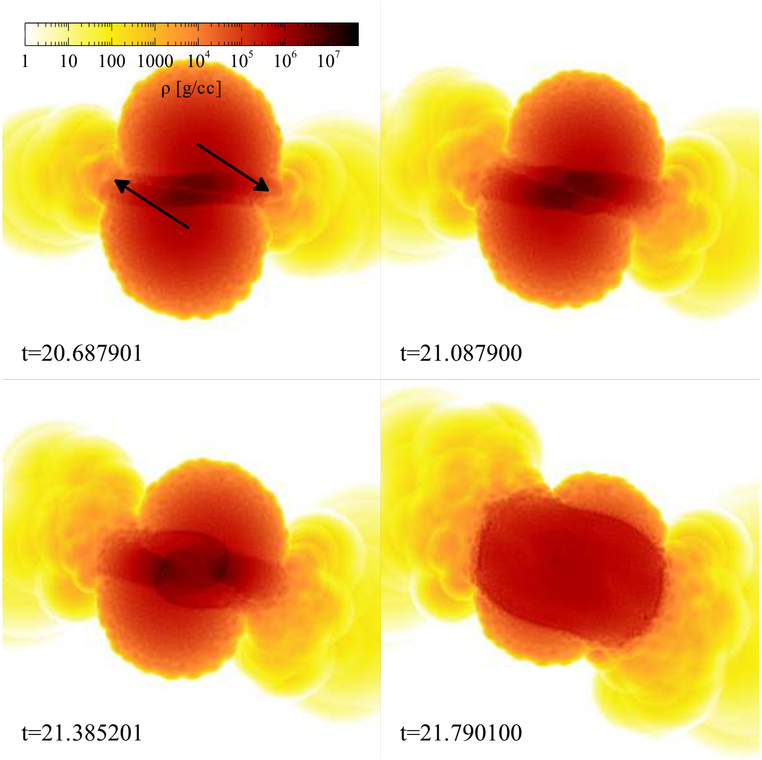

Raskin et al 2010

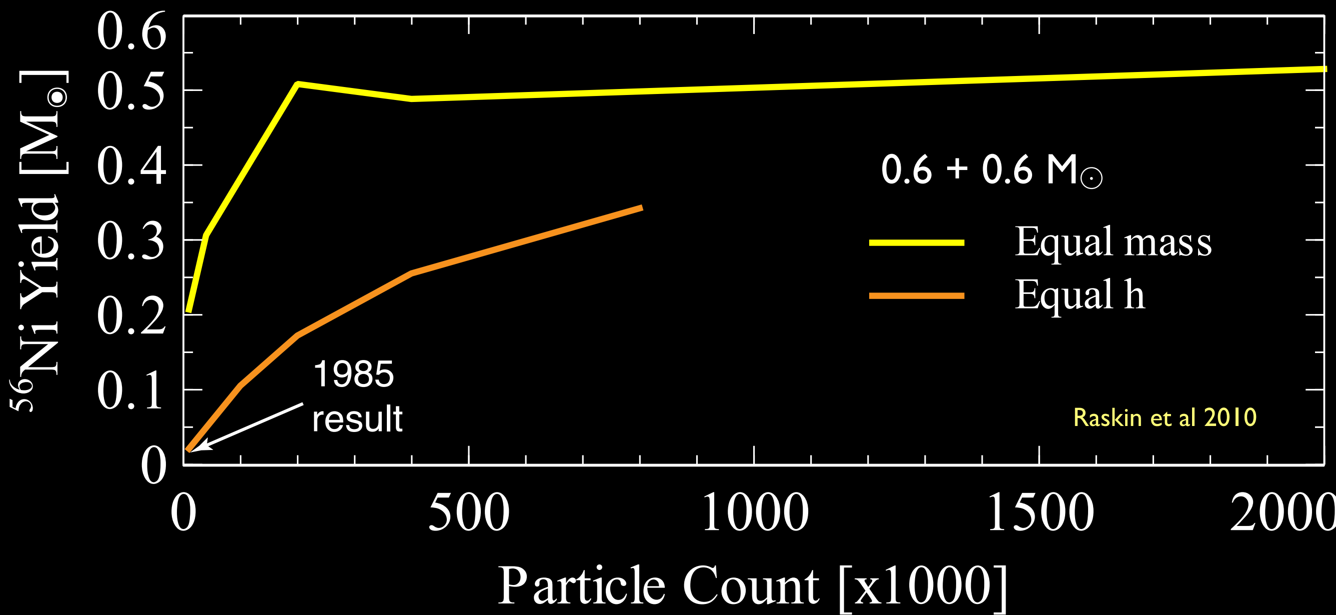

0.6 + 0.6 M☉
Equal mass
Equal h
1985
result
Raskin et al 2010
56Ni Yield [M☉]
Particle Count [x1000]
0
0.1
0.2
0.3
0.4
0.5
0.6
0
500
1000
1500
2000

Advances (plus a little serendipity) over the next decade should enable us to decipher the progenitors of white dwarf supernovae:

1) Silicon, Sulfur, Calcium ratios
2) Unburned carbon and oxygen
3) Tidal tails
4) Sufficient number of binary WDs
5) Early gamma-rays
6) Narrow hydrogen emission or absorption
7) Circumstellar interaction in radio or x-rays
8) Gravitational wave signatures
9) Frequency as a function of redshift